Mon. Not. R. Astron. Soc. **341,** 385–404 (2003)

# On the formation and evolution of black hole binaries

Ph. Podsiadlowski,[1⋆] S. Rappaport[2] and Z. Han[3]

[1] *University of Oxford, Department of Astrophysics, Oxford OX1 3RH*
[2] *Department of Physics and Centre for Space Research, Massachusetts Institute of Technology, Cambridge, MA 02139, USA*
[3] *Yunnan Observatory, National Astronomical Observatories, the Chinese Academy of Sciences, Kunming 650011, China*

Accepted 2003 January 24. Received 2002 November 1; in original form 2002 July 8

**ABSTRACT**

We present the results of a systematic study of the formation and evolution of binaries containing black holes and normal-star companions with a wide range of masses. We first reexamine the standard formation scenario for close black hole binaries, where the progenitor system, a binary with at least one massive component, experienced a common-envelope phase and where the spiral-in of the companion in the envelope of the massive star caused the ejection of the envelope. We estimate the formation rates for different companion masses and different assumptions about the common-envelope structure and other model parameters. We find that black hole binaries with intermediate- and high-mass secondaries can form for a wide range of assumptions, while black hole binaries with low-mass secondaries can only form with apparently unrealistic assumptions (in agreement with previous studies).

We then present detailed binary evolution sequences for black hole binaries with secondaries of 2 to 17 $M_\odot$ and demonstrate that in these systems the black hole can accrete appreciably even if accretion is Eddington-limited (up to 7 $M_\odot$ for an initial black hole mass of 10 $M_\odot$) and that the black holes can be spun up significantly in the process. We discuss the implications of these calculations for well-studied black hole binaries (in particular GRS 1915+105) and ultraluminous X-ray sources of which GRS 1915+105 appears to represent a typical Galactic counterpart. We also present a detailed evolutionary model for Cygnus X-1, a massive black hole binary, which suggests that at present the system is most likely in a wind mass-transfer phase *following* an earlier Roche-lobe overflow phase. Finally, we discuss how some of the assumptions in the standard model could be relaxed to allow the formation of low-mass, short-period black hole binaries, which appear to be very abundant in nature.

**Key words:** black hole physics – gravitation – binaries: close – stars: individual: Cygnus X-1 – stars: individual: GRS 1915+105 – X-rays: stars.

## 1 INTRODUCTION

There are currently 17 binary systems containing black holes for which dynamical mass estimates are available (see e.g. table 1 of Lee, Brown & Wijers (2002) [LBW], and references therein; Orosz et al. 2002). According to conventional wisdom, these systems formed from primordial binaries where at least one of the stars was quite massive (i.e. $M \gtrsim$ 20–25 $M_\odot$). If mass transfer from the primary to the secondary commences at an orbital period in the range of ∼1–10 yr, a common envelope may form during which the hydrogen-rich envelope of the primary is expelled (Paczyński 1976). If the secondary and the core of the primary avoid a merger, then the massive core may evolve to core collapse and the formation of a black hole in a close binary.

For nine of the 17 black hole binaries (see e.g. LBW), the current-epoch companion mass is $\lesssim$1 $M_\odot$ and the orbital periods are $\lesssim$ 1 d. For reasons discussed later in the text, these systems probably had primordial secondaries whose mass was not substantially greater than ∼1.5 $M_\odot$ (but see Section 4.4). One quantitative difficulty with the common-envelope scenario for forming this type of black hole binary is that the amount of orbital energy that can be released by the spiral-in of a low-mass secondary may not be sufficient to eject the massive envelope of the primary. It has long be recognized that this is energetically challenging even if the common-envelope ejection mechanism is very efficient (Podsiadlowski, Cannon & Rees 1995; Portegies Zwart, Verbunt & Ergma 1997; Kalogera 1999; see, however, also Romani 1992). Furthermore, recent determinations of the binding energy of the envelopes of massive supergiants by Dewi & Tauris (2000, 2001) suggest that all studies so far may have significantly underestimated how tightly bound these envelopes actually are, which seriously aggravates the problem. On

⋆E-mail: podsi@astro.ox.ac.uk

the other hand, it has been estimated that there may be up to several thousand low-mass black hole transients in the Galaxy (Wijers 1996; Romani 1998). This has led to several alternative formation scenarios for low-mass black hole binaries, where either the low-mass companion is a third star in a triple system being captured into a tight orbit when the two massive components merge (Eggleton & Verbunt 1986), or where the low-mass star forms after the black hole – out of a collapsed massive envelope (Podsiadlowski et al. 1995). In the present work we reexamine the standard formation scenarios for low-mass black hole binaries with plausible modifications to some of the usual assumptions.

By contrast, for four of the black hole binaries, the mass of the companion is substantially larger (i.e. $\gtrsim 6\,M_\odot$), and the availability of orbital binding energy for ejecting the common envelope is greatly enhanced. The remaining 4 systems (4U 1543-47, GRO J1655-40, GS 2023+338, and GRS 1915+105) have either intermediate-mass donor stars (i.e. $2 \lesssim M_{\rm d} \lesssim 5\,M_\odot$) or orbital periods longer than 2.5 d, thereby allowing for primordial secondaries of at least intermediate mass, and substantial mass loss or evolution of the secondary to its present status as the donor star. It is on the evolution of these latter two categories, with particular emphasis on GRS 1915+105, that we focus this work (for other recent discussions of intermediate-mass black hole binaries see Kalogera 1999; Brown et al. 2000; LBW).

In addition to the common-envelope ejection mechanism, another major uncertainty in the modelling of black hole binaries is the initial mass of the black hole which is caused by uncertainties in the theory of both single and binary stellar evolution. Some of the key factors that determine the maximum initial black hole mass are (1) the minimum initial mass above which a star leaves a black hole remnant (mostly believed to be in the range of 20–25 $M_\odot$; Maeder 1992; Woosley & Weaver 1995; Portegies Zwart et al. 1997; Ergma & Fedorova 1998; Ergma & van den Heuvel 1998; Brown et al. 2000; Fryer & Kalogera 2001; Nelemans & van den Heuvel 2001; cf. Romani 1992), (2) the minimum mass above which a single star loses its envelope in a stellar wind and becomes a helium/Wolf–Rayet star, (3) the maximum radius of a single star before and after helium core burning, (4) the amount of wind mass loss in the Wolf–Rayet phase and (5) the fraction of the mass that is ejected when the black hole forms (for detailed recent discussions see Brown et al. 2000; Fryer & Kalogera 2001; Nelemans & van den Heuvel 2001). Generally one expects the most massive black holes to form from stars that have an initial mass close to the minimum mass above which a star loses its hydrogen-rich envelope in a stellar wind and becomes a Wolf–Rayet star, and where the common-envelope phase occurs near the end of the evolution of the massive primary (i.e. experiences case C mass transfer; Brown, Lee & Bethe 1999; Wellstein & Langer 1999). This avoids a long phase where the mass of the helium star, the black hole progenitor, is reduced by a powerful stellar wind, as typically seen from Wolf–Rayet stars, which would reduce the final helium star mass and hence the maximum black hole mass (see e.g. Woosley, Langer & Weaver 1995).[1] Unfortunately, the evolutionary tracks for massive post-main-sequence stars and in particular the maximum radius a star attains after helium core burning are rather uncertain (and generally inconsistent with observed distributions of stars in the Hertzsprung–Russell diagram; see e.g. Langer & Maeder 1995). Fryer & Kalogera (2001) have shown that initial black hole masses as high as 15 $M_\odot$ can be obtained if either the parameter range for case C mass transfer is increased or the wind mass-loss rate in the helium star phase of the black hole progenitor is reduced (see also Brown et al. 2001; Nelemans & van den Heuvel 2001; Belczynski & Bulik 2002; Pols & Dewi 2002).

Only a few of the previous studies (e.g. LBW) have considered the possibility that the black hole may increase its mass substantially since its formation by mass transfer from the companion star. It is one of the purposes of this paper to demonstrate that accretion from a companion star can substantially increase the mass of a black hole and spin it up in the process and that the present mass may not be representative of the initial black hole mass. A closely coupled result is that the observed donor star masses may be substantially lower than their initial mass.

The paper is structured as follows. In Section 2 we present detailed binary population synthesis calculations to show how the formation rate of black hole binaries and the distribution of the secondary masses depend on the structure of massive supergiant envelopes and the modelling of common-envelope ejection. In Section 3 we discuss the results of extensive binary evolution calculations for black hole binaries with intermediate-/high-mass secondaries, which we then apply in Section 4 to observed systems, in particular GRS 1915+105, ultraluminous X-ray sources and Cyg X-1. Finally, in Section 4 we reexamine the standard formation scenario for low-mass black hole binaries to understand why such systems appear to be so plentiful in nature.

## 2 BINARY POPULATION SYNTHESIS MODEL

### 2.1 Assumptions of the model

In this work we consider only black hole binaries that descend from a primordial binary pair of stars. Black-hole binaries that may form dynamically in globular clusters are left for another study. We start our investigation of black hole binaries, which includes (initially) intermediate- and high-mass donors, by carrying out a Monte Carlo population study aimed at producing systems at the end of the common-envelope phase. This will provide guidance for the second part of our study where we follow in detail the X-ray binary phase which involves mass transfer from the donor star to the black hole.

The assumptions and ingredients that we adopt for the population study are listed below. For prior studies of the formation and evolution of black hole binaries see e.g. Romani (1992), Portegies Zwart et al. (1997), Ergma & van den Heuvel (1998), Ergma & Fedorova (1998), Kalogera (1999), Brown et al. (2000) and Fryer & Kalogera (2001); also see Kalogera & Webbink (1998) for a related, detailed study of the theoretical constraints on the formation of neutron-star X-ray binaries.

We utilize a simple power-law distribution for the initial mass function (IMF) for the primary stars in primordial binaries. Specifically, we take $\mathrm{d}N/\mathrm{d}M_{\rm p} \propto M_{\rm p}^{-x}$ with $x = 2.35$ (Salpeter 1955). Since we consider a relatively small range of primary masses, the results are not very sensitive to the particular choice of $x$ or to the fact that the IMF flattens significantly toward lower masses (see e.g. Miller & Scalo 1979). Only primordial binaries with mass $M_{\rm p} > 25\,M_\odot$ are considered as progenitors of black holes. This lower limit is somewhat uncertain, but is consistent with current models of massive stars and the modelling of supernova explosions (e.g. Woosley & Weaver 1995; Fryer & Kalogera 2001). We also

[1] It should also be noted that in the formation of some black holes (e.g. the black hole in Nova Scorpii) a significant fraction of the mass of the helium star is ejected in the supernova explosion in which the black hole formed (Podsiadlowski et al. 2002; LBW). Thus the final helium star mass strictly provides only an upper limit on the black hole mass.

somewhat arbitrarily take the upper mass limit for the primary to be $M_{\rm p} < 45\ {\rm M}_{\odot}$.

The mass of the secondary star, $M_{\rm s}$, in the primordial binary is chosen from a flat mass ratio distribution, i.e. $f(q) = 1$, where $q \equiv M_{\rm s}\ /M_{\rm p}$. There is a large degree of uncertainty in the actual distribution of mass ratios in binaries; however, our choice reflects the simple fact that a significant fraction of high-mass stars are observed to have high-mass companions (see e.g. Garmany, Conti & Massey 1980). At the low-mass end, only secondaries with mass $M_{\rm s} \gtrsim 0.5\ {\rm M}_{\odot}$ are retained in the population synthesis.

The orbital period distribution of primordial binaries is taken to be constant in $\log P_{\rm orb}$, where $P_{\rm orb}$ is the orbital period (see e.g. Abt & Levy 1978). While orbital eccentricity among primordial binaries might be expected to have a distribution that increases linearly with $e$ (Duquennoy & Mayor 1991), we have simply taken all orbits to be circular. One motivation for this choice is that the tidally circularized orbital radius of an eccentric binary is $(1 - e^2)a$, which we note is simply linearly proportional to $a$, the initial orbital semimajor axis. Thus, the distribution in circularized orbital radii would be the same as that for the semimajor axes, regardless of the distribution in $e$, as long as that distribution is independent of $a$.

The evolution of the primary star as it expands toward filling its Roche lobe is followed with the Hurley, Pols & Tout (2000, hereafter HPT) code. The evolution includes wind mass loss from the primary according to the prescription of Nieuwenhuijzen & de Jager (1990). These stars have fully developed core masses given by $M_{\rm core} \simeq 0.12\ M_{\rm p}^{1.35}$ (in solar masses; see e.g. HPT). Typical wind mass losses prior to the primary traversing the Hertzsprung gap (hereafter HG) amount to only $\sim$2–6 $\rm M_{\odot}$; however, much larger losses can be sustained once stellar radii of $\gtrsim$1000 $\rm R_{\odot}$ are reached. In this latter regard, we compute the orbital widening owing to the stellar wind mass loss according to ${\rm d}a/a = -{\rm d}M_{\rm w}/M_{\rm b}$, where the fractional change in orbital separation is equal to the wind mass loss from the primary (d $M_{\rm w}$) divided by the total mass of the binary, $M_{\rm b}$. This expression is based only on the assumption that the specific angular momentum carried away by the wind is equal to that of the primary star in the binary orbit (see, however, the discussion in Section 4.4).

An interesting possibility occurs if the initial Roche-lobe radius, $R_{\rm L}$, of the primary falls in the range $R_{\rm HG} < R_{\rm L} < R_{\rm max}$, where $R_{\rm HG}$ is the stellar radius at the end of the Hertzsprung gap, and $R_{\rm max}$ is the maximum radius that the primary can attain. It is in this phase of the evolution that the primary can lose a substantial fraction of its envelope mass in a stellar wind, thereby requiring less orbital binding energy to eject the remaining envelope of the primary once mass transfer commences (see the discussion below). However, as the primary expands and loses mass in a wind, the mass loss also causes the orbit to expand (as described above). It it therefore not obvious whether the expanding star can catch up with its Roche lobe. To quantify this issue, we first define a Roche-lobe index due to wind loss:

$$\xi_{\rm L,w} \equiv \left(\frac{{\rm d}\ln R}{{\rm d}\ln M_{\rm b}}\right)_{\rm L,w} \simeq 1 - \left(\frac{0.087}{r_{\rm L}}\right)\left(\frac{M_{\rm b}}{M_{\rm p}}\right) \qquad (1)$$

as well as a stellar index associated with wind mass loss:

$$\xi_{*,\rm w} \equiv \left(\frac{{\rm d}\ln R}{{\rm d}\ln M_{\rm b}}\right)_{*,\rm w} \simeq (0.023 + 0.00086[30 - M_{\rm HG}])M_{\rm b}, \qquad (2)$$

where $M_{\rm b}$ is the instantaneous total mass of the binary (including wind mass loss), $M_{\rm HG}$ is the mass of the primary at the end of the Hertzsprung gap (both in solar masses), and $r_{\rm L}$ is the Roche-lobe radius of the primary in units of the orbital separation. In both cases, a minus sign has been subsumed into the definition of d $M_{\rm w}$ since it is always negative. The above expressions for $\xi_{*,\rm w}$ and $\xi_{\rm L,w}$ were derived from fits to the stellar models in HPT and the expression for the Roche-lobe radius of Plavec (1968), respectively. If $\xi_{*,\rm w} < \xi_{\rm L,w}$ when the primary expands past the HG, then it will never catch up with its Roche lobe since $\xi_{*,\rm w}$ decreases faster with mass loss than does $\xi_{\rm L,w}$ (this catch-up problem has first been identified by Kalogera & Webbink 1998 in their study of the formation of neutron-star X-ray binaries). We have found that even if the reverse inequality holds when the primary expands past the HG, it is still extremely rare for the star to overtake its Roche lobe.

If the primary does evolve to the point of overflowing its Roche lobe (almost always before the end of the HG), we use a simple prescription for deciding whether a common-envelope phase ensues. If the primary has evolved at least to the start of the Hertzsprung gap and the mass ratio $M_{\rm p}/M_{\rm s}$ exceeds 2.0, or if the primary is beyond the HG and the mass ratio exceeds a value of 1.2, we assume that a common envelope will occur. For other conditions we take the mass transfer to be quasi-conservative and stable. These latter systems are not very common and do not lead to the type of black hole binary that we are considering.

A commonly used prescription was employed to determine the orbital separation after the common-envelope phase (see e.g. de Kool (1990); Dewi & Tauris 2000):

$$\left(\frac{a_{\rm f}}{a_{\rm i}}\right)_{\rm CE} = \frac{M_{\rm c}M_{\rm s}}{M_{\rm p}}\left(M_{\rm s} + \frac{2M_{\rm e}}{\alpha_{\rm CE}\lambda r_{\rm L}}\right)^{-1}, \qquad (3)$$

where the subscripts $f$ and $i$ denote the final and initial values, respectively, $M_{\rm c}$ and $M_{\rm e}$ are the core and envelope masses of the primary, respectively, $\alpha_{\rm CE}$ is the efficiency with which the orbital binding energy can liberate the envelope of the primary, $\lambda^{-1}$ is the energy of the envelope of the primary in units of $-GM_{\rm p}M_{\rm e}/R_{\rm p}$, and $r_{\rm L}$ is the dimensionless Roche-lobe radius of the primary.

Appropriate values of the $\lambda$ parameter are derived from stellar structure and evolution calculations (with similar assumptions as in HPT and wind mass loss according to Nieuwenhuijzen & de Jager 1990) that we have carried out specifically for this work. These results are shown in Fig. 1, where the definition for $\lambda$ in the left panel includes only the gravitational binding energy ($\lambda_{\rm gr}$), while in the panel on the right it also includes the thermal and the ionization energy ($\lambda_{\rm tot}$; see Han, Podsiadlowski & Eggleton 1994; Dewi & Tauris 2000). We have compared these curves with those computed by Dewi & Tauris 2000, 2001 and found them to be in reasonable agreement at similar evolutionary stages, although the evolutionary tracks are slightly different. We note that the value of $\lambda$ itself depends to some degree on the definition of the core–envelope boundary (see Han et al. 1994; Tauris & Dewi 2001). Here we have defined the core mass as the central mass that contains $1\ {\rm M}_{\odot}$ of hydrogen (in contrast Dewi & Tauris (2000) defined it as the central mass which includes 10 per cent of the total mass of hydrogen). In agreement with Tauris & Dewi 2001 we find that in some evolutionary phases the value of $\lambda$ can be a rather sensitive function of the chosen core–envelope boundary; this is particularly true for very evolved supergiants near the end of their evolution. Unfortunately, this uncertainty in the definition of $\lambda$ cannot easily be resolved without a better understanding of the CE ejection process.

Values of $\lambda_{\rm tot}$ that are appropriate to stars in the mass range 25–45 $\rm M_{\odot}$ and the later phases of their evolution (i.e. in or beyond the HG) lie in the range of $0.01 \lesssim \lambda \lesssim 0.06$. Note that for a 20 $\rm M_{\odot}$ model $\lambda$ increases to a value $\sim$1 near the very end of the evolution. This occurs when the star ascends the asymptotic giant branch and develops a deep convective envelope, creating a steep chemical

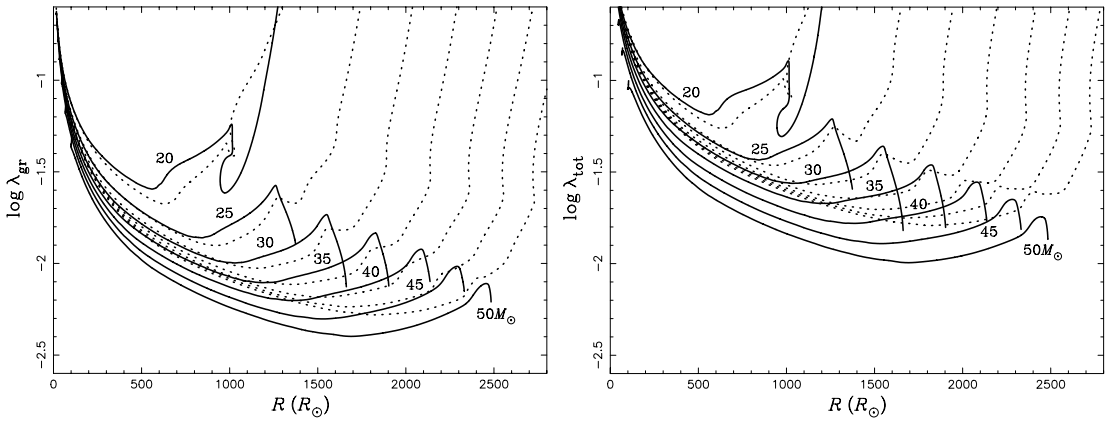


**Figure 1.** The envelope structure parameter λ as a function of stellar radius for different masses as indicated after hydrogen has been exhausted in the core. In the panels on the left, λ only includes the gravitational binding energy, while on the right λ includes both the gravitational and the thermal energy (similar to Dewi & Tauris (2000)). The dotted curves are calculated without inclusion of a stellar wind. Note that in this case λ always becomes large at the largest radii attained by the models.

gradient ($\mu$ gradient) below the convective envelope (i.e. establishes a typical giant structure). The more massive stars experience a supernova before this phase is reached. Since these results depend on the assumptions in the stellar modelling, we also performed a series of calculations without any wind mass loss, shown as dotted curves in Fig. 1. The models now achieve significantly larger radii, and λ increases dramatically near the end of the evolution in all cases. This demonstrates that the behaviour of λ is also quite sensitive to uncertainties in the stellar modelling itself, adding another uncertainty to the problem. In view of these uncertainties we adopted a value of λ in this work that is held constant throughout the evolution of a star. We were careful, however, to test the full range of plausible values for λ (0.01–0.5).

The value for $\alpha_{\rm CE}$ was simply taken to be unity. Since the two parameters $\alpha_{\rm CE}$ and λ appear as a product in the expression for the post-CE orbital separation, the uncertainty in one can, to some degree, be incorporated into the uncertainty in the other. A value of $\alpha_{\rm CE} \sim 1$ was motivated by a number of recent empirical studies of the efficiency of the CE ejection process which have suggested that the CE ejection process must be very efficient; see e.g. the recent study of sdB stars in compact binaries by Han et al. (2002, 2003) (these are short-period binaries that have formed through a very well defined CE channel and are hence particularly suitable for studying the CE ejection process empirically). In their best model, these authors found $\alpha_{\rm CE} = 0.75$ and that ∼75 per cent of the thermal energy of the envelope had to be used in the ejection process to explain the observed orbital period distribution of compact sdB binaries. However, this empirical study, as well as all other previous ones, strictly apply only to systems where the donor is a giant with a convective envelope but not to systems which experience a CE phase when the donor star is in the Hertzsprung gap and has a radiative envelope. Such stars have fundamentally different internal structures and are much more centrally concentrated than more evolved (super-)giants with convective envelopes (see e.g. fig. 2 in Podsiadlowski 2001) (this is e.g. reflected in the low value of λ for stars in the Hertzsprung gap in Fig. 1). In such systems, the core–envelope separation may not be distinct enough to allow envelope ejection even if enough energy is available in principle (see e.g. Taam & Sandquist 2000; and Kalogera, private communication); hence a value of $\alpha_{\rm CE} \sim 1$ may not be an appropriate one for systems that experience a CE phase in the Hertzsprung gap.

Immediately after the common-envelope phase has occurred, we check whether the secondary star is overfilling its Roche lobe. If so, we assume that the secondary merges with the core and do not follow the binary further.

The amount of wind mass loss from the exposed H-exhausted core of the primary as it evolves toward core collapse is quite uncertain. To cover a full range of possibilities we adopt the following somewhat ad hoc prescription for the mass of the black hole that eventually forms from the collapse: $M_{\rm BH} = 6{\rm M}_\odot + (M_{\rm He} - 6{\rm M}_\odot)\mathcal{R}$, where $M_{\rm He}$ is the mass of the newly exposed H-exhausted core, and $\mathcal{R}$ is a uniform random variable between 0 and 1. With this prescription we produce black holes of mass over the range of ∼6–20 $\rm M_\odot$. The orbital separation at the end of this wind loss phase is taken to be a factor of $(M_{\rm He} + M_{\rm s})/(M_{\rm BH} + M_{\rm s})$ larger than the separation at the end of the common-envelope phase (see the expression above for the change in orbital separation with wind mass loss). We specifically chose this procedure to obtain black hole masses that are reasonably consistent with the observed ones (e.g. Fryer & Kalogera 2001; van den Heuvel 2001, LBW), but also to avoid some of the theoretical uncertainties that lead to these masses (e.g. the wind mass-loss rate in the helium star phase, the question of case B versus case C mass transfer; see the discussion in Section 1). If it is indeed necessary that systems with relatively massive black holes have experienced case C mass transfer in the past (e.g. Brown et al. 1999; Wellstein & Langer 1999; Langer 2002, private communication), our procedure implicitly assumes that those evolutionary tracks for single stars which presently do not allow case C mass transfer for stars more massive than ∼20 $\rm M_\odot$ are not correct (also see Fryer & Kalogera 2001). Note also that our procedure does not produce relatively low-mass black holes with masses <6 $\rm M_\odot$ which could have a somewhat different evolution from the black hole systems studied in this paper (see Fryer & Kalogera 2001; Beer & Podsiadlowski 2002).

When the evolving He star undergoes core collapse, we assume that the entire mass of the He star collapses into the newly formed black hole (but see LBW), and that there is no natal 'kick' imparted to the black hole. Much has been inferred about natal kicks to neutron stars from the proper motions of radio pulsars and from studies of numerous individual binary systems containing neutron stars (see e.g. Lyne & Lorimer 1994; Brandt & Podsiadlowski 1995; Verbunt & van den Heuvel 1995; Hansen & Phinney 1997; van den Heuvel

et al. 2000; Arzoumanian, Chernoff & Cordes 2002). Yet, relatively little is understood about the physical origin of these kicks or the conditions under which kicks are developed (see e.g. Janka & Müller 1994; Fryer, Burrows & Benz 1997; Spruit & Phinney 1998; Fryer & Heger 2000; Lai, Chernoff & Cordes 2001; Pfahl et al. 2002). Unfortunately, even less is known about the nature of natal kicks delivered to forming black holes. The spatial distribution and the kinematics of the majority of black hole binaries appear to be consistent with the assumption that no asymmetric kicks are imparted to the black hole (Brandt, Podsiadlowski & Sigurdsson 1995; White & van Paradijs 1996), although there is at least one clear exception (the black hole in Nova Sco; Brandt et al. 1995; Fryer & Kalogera 2001; Podsiadlowski et al. 2002a; for a different view see Nelemans, Tauris & van den Heuvel 1999).

In order to compute an absolute formation rate for black hole binaries in the binary population synthesis (hereafter BPS; see next section), we take the birth rate of stars with mass $\gtrsim 8$ M$_\odot$ to be 1 per 100 yr, to match the Galactic supernova rate [of non-type Ia supernovae (SNe); see e.g. Cappellaro, Evans & Turatto (1999)]. This rate, coupled with the assumed slope of the IMF, yields a maximum potential formation rate for black hole primordial binaries of $\sim 6 \times 10^{-4}$ yr$^{-1}$; this includes an approximate fraction for stars born in binaries of $\sim$1/2.

Finally, we note that once the incipient black hole binaries have been produced, the luminous X-ray phase will not start until the secondary has evolved to either produce a strong stellar wind or overflow its Roche lobe. In the BPS portion of this work we carry the calculations only to the point of the successful ejection of the common envelope or merger of the secondary with the core of the primary. We also apply a very simplistic check for the dynamical stability of mass transfer when the donor star ultimately commences mass transfer via Roche lobe overflow on to the black hole. Here we required that $M_s \lesssim M_{BH}$; however, we note that in the detailed binary evolution calculations presented in Section 3, the stability of the mass transfer is calculated self-consistently in each evolution step, and that even higher mass donor stars may result in stable mass transfer. The successful incipient black hole binaries are tabulated and statistical results are extracted.

Many of the above assumptions regarding the formation of black hole binaries are discussed in further detail by Romani (1992), Portegies Zwart et al. (1997), Ergma & van den Heuvel (1998), Ergma & Fedorova (1998), Kalogera (1999), Brown et al. (2000) and Fryer & Kalogera (2001). One substantive difference in the assumptions that we make in comparison with those utilized in prior work is that we do *not* set any a priori restrictive upper limit on the mass of the donor star in the incipient black hole binary. Also, the values for $\lambda$ that we use are considerably smaller (by up to a factor of $\sim$20) than the values employed in most earlier work. Smaller values of $\lambda$ require the expenditure of more orbital binding energy to successfully eject the common envelope. Finally, we do *not* require that the donor star be unevolved when it commences mass transfer on to the black hole (cf. Kalogera 1999). This is due to the fact that we explicitly include wide binaries containing black holes.

### 2.2 Binary population synthesis results

Each binary population synthesis run (BPS) was typically started with $\sim 10^7$ primordial binaries, all of which have $M_p > 25$ M$_\odot$. Each binary is followed using the prescriptions, assumptions, and algorithms specified in the previous section, until it either becomes an incipient black hole X-ray binary or goes down an alternate evolutionary path. The relevant binary parameters are stored for each 'successful' system.

Illustrative results from a BPS run with the $\lambda$-parameter set equal to 0.5, a conventionally used value, are shown in Fig. 2(a). Each dot in the $P_{orb}$–$M_{d,i}$ plane represents a single incipient black hole X-ray binary just after the black hole has been formed; $P_{orb}$ is the orbital period and $M_{d,i}$ is the initial mass of the donor star. The number of primordial binaries used in this run was limited to only $1.5 \times 10^6$ in order to keep the density of points legible in the figure. The sharp lower boundary in Fig. 2(a) results from the fact that systems with shorter orbital periods have merged, i.e. the donor star overflowed its critical potential lobe at the end of the common-envelope phase. The filled circles are starting models for the detailed evolutionary calculations of the binary X-ray phase presented in Section 3.

In all, there are about 25 000 dots in Fig. 2(a), each representing the successful formation of an incipient black hole binary X-ray source. The expression we use to convert this number, $N$, to a formation rate is as follows:

$$R = \left(\frac{1}{2}\right)\left(\frac{1}{8}\right)\left(\frac{N}{N_0}\right)\tau_{SN}^{-1} \quad (4)$$

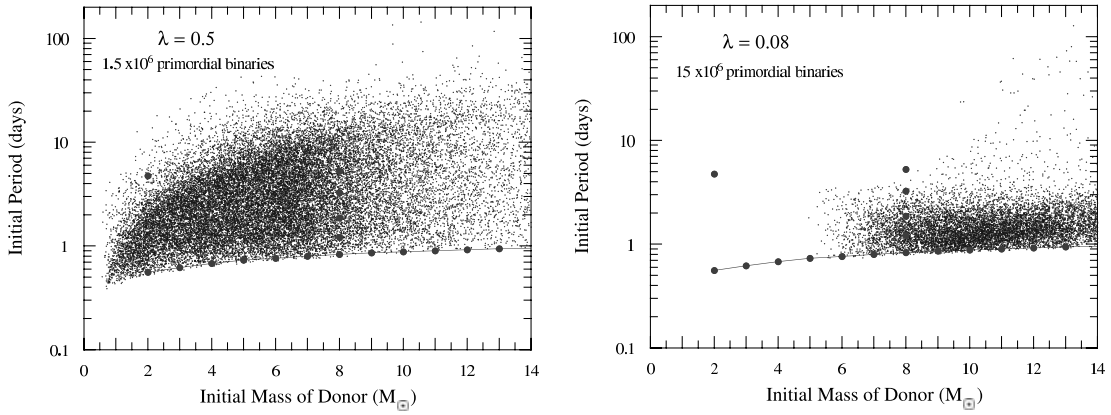


**Figure 2.** Distribution of initial orbital period and initial secondary mass for black hole binaries at the beginning of mass transfer for different assumptions about the common-envelope (CE) structure and ejection efficiency, characterized by the parameters $\lambda$ and $\alpha_{CE}$, respectively, where $E^{CE}{}_{env} = GM_e\, M_p\, /\lambda\, R_p$ is the binding energy of the envelope. The value of $\alpha_{CE}$ was fixed as 1, while two different illustrative values of $\lambda$ were used to produce the right and left panels. The solid circles indicate the initial positions of our detailed binary evolution sequences which are discussed in Section 3. This figure is available in colour in the online version of the journal on *Synergy*.

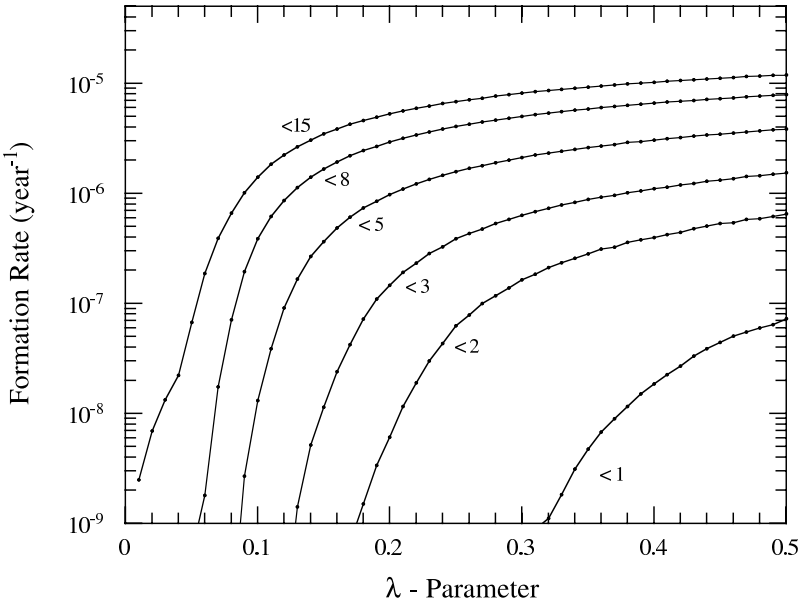


**Figure 3.** Formation rate of black hole binaries as a function of the envelope structure parameter λ. The different curves assume a different maximum mass for the secondary (in $M_\odot$), as indicated along the respective curves. This figure is available in colour in the online version of the journal on *Synergy*.

where $N_0$ is the starting number of primordial binaries (with $M_p > 25\ M_\odot$), the factor of 1/2 is an approximation to the fraction of stars born in binaries, the factor of 1/8 represents the fraction of stars capable of collapsing to a neutron star or black hole that comes from the mass range 25–45 $M_\odot$, and $\tau^{-1}{}_{SN}$ is the Galactic supernova rate (of non-type Ia SNe; see discussion above). The factor of 1/8 depends somewhat, but not sensitively, on the slope of the IMF. The particular example shown in Fig. 2(a) then implies a formation rate for such systems of $\sim 1 \times 10^{-5}\ yr^{-1}$.

A second illustrative example of a BPS run is shown in Fig. 2(b) for the case where the λ parameter has been reduced to 0.08. The number of primordial binaries in this run was 10 times that used in Fig. 2(a). In spite of this, the number of systems represented in Fig. 2(b) is actually fewer than in Fig. 2(a) due to the highly reduced formation efficiency associated with the lower value of λ. Note that, in addition to the overall drop in formation efficiency, there is a complete dearth of systems with donor masses of $\lesssim 5\ M_\odot$. This results from the fact that for small values of λ (i.e. more envelope binding energy) the systems with lower mass donor stars do not have sufficient orbital energy to unbind the common envelope.

We have systematically investigated the effect of λ on the formation efficiency of incipient black hole binaries. The BPS code was run for 50 values of λ in the range of 0.01–0.5, in steps of 0.01, and a formation efficiency computed for each. The results, shown in Fig. 3, are further broken down according to the donor masses contributing to the population. The top curve shows the formation rate for systems with all donor masses ($<15\ M_\odot$) computed according to equation (4). Note the abrupt drop in formation rate for values of $\lambda \lesssim 0.1$. The sequence of curves below this is for the formation rate of black hole X-ray binaries with donor masses <8, <5, <3, <2, and $<1\ M_\odot$, respectively. The small shoulder on the curve for $<15\ M_\odot$ at very small values of λ results from Roche-lobe overflow when the primary has evolved beyond the HG and has lost a significant amount of its envelope to a stellar wind. Two immediate conclusions to be drawn from the results in Fig. 3 are: (1) black hole binaries with low *incipient* donor masses (i.e. $\lesssim 1\ M_\odot$) have extremely low formation rates unless either seemingly unphysical (large) values of λ are invoked or much lower mass primary stars are able to form black holes (see e.g. Portegies Zwart et al. 1997; Kalogera 1999); and (2) the formation rates for black hole binaries with *incipient* intermediate-mass donor stars can be quite substantial provided that the λ parameter is not smaller than ∼0.1.

In addition to the BPS results shown in Fig. 3 we have carried out some additional studies of how the theoretical uncertainties in the values of λ affect our conclusions. As can be seen from Fig. 1, the values of λ depend systematically on the stellar mass, with the larger values (smaller envelope binding energies) generally being associated with the lower masses. Since, to this point, we have excluded primary masses below 25 $M_\odot$, and these have the largest values of λ, we have carried out an additional sequence of BPS calculations with the inclusion of 20–25 $M_\odot$ primaries to test whether these would significantly enhance the formation rate of black hole binaries. Here, we simply recomputed the formation rates, as in Fig. 3, but now with the minimum primary mass set to 20 $M_\odot$. Again, for the purposes of the BPS calculations, we took the value of λ to be fixed for primaries of all masses and evolutionary states, and studied how the formation rates changed with a systematic variation in the adopted value of λ. The result is that for any given value of λ, the rates are larger than those shown in Fig. 3 by a factor typically limited to ∼1.5. This is a bit less than might be expected simply from the increased primary mass range – weighted by the Salpeter mass function. The smaller than anticipated increase is due to the fact that many of the systems produced by ∼20-$M_\odot$ primaries have relatively low-mass black holes and the subsequent mass transfer is unstable.

Finally, we constructed from the results of Fig. 1 a simple dependence of the λ parameter on primary mass: $\lambda = \lambda_0 \exp(-0.074[M_p - 20\ M_\odot])$, where $\lambda_0$ is a constant to be supplied. For the 'plateau' regions in Fig. 1(b), the value of $\lambda_0$ would be approximately 0.08. We then produced a sequence of BPS runs, including primary masses down to 20 $M_\odot$, where the value of $\lambda_0$ was varied systematically over the range of 0.01–0.5. Thus, for any given choice of $\lambda_0$, in a given BPS run, the values of λ used scale with primary mass as in the exponential expression given above. The net result of this study, as expected, is that the formation rates are all systematically *reduced* compared with the values shown in Fig. 3 where a fixed value of λ

was utilized in each BPS run. The reason for this reduction in formation rates is that now $\lambda_0$ represents an upper limit to the value of $\lambda$ (corresponding to 20-$M_\odot$ stars), with all higher-mass stars having smaller values of $\lambda$.

The conclusion drawn from these experiments, that extend the primary masses down to 20 $M_\odot$ and compute $\lambda$ from a prescription that depends on the primary mass, is that the rates shown in Fig. 3 are, to within a factor of a few, likely to be *upper limits.*

## 3 BINARY EVOLUTION CALCULATIONS

In this section we present a series of binary stellar evolution calculations to illustrate the evolution of black hole binaries with intermediate- and high-mass secondaries. In Section 3.1 we briefly describe the binary evolution code and the main assumptions used in the calculations, and in Section 3.2 we present the main results of the calculations. In the subsequent section we will apply these results to a variety of systems.

### 3.1 Description of the code and principal assumptions

All our calculations were performed with a standard Henyey-type stellar evolution code (Kippenhahn, Weigert & Hofmeister 1967) which we have used in various similar investigations in the past and which is described in detail in PRP Podsiadlowski, Rappaport & Pfahl (2002b, hereafter PRP). It uses up-to-date stellar OPAL opacities (Rogers & Iglesias 1992), complemented with those by Alexander & Ferguson (1994) at low temperatures. In all calculations we assumed an initial solar composition with $X = 0.70$ and $Z = 0.02$, took a mixing-length parameter $\alpha = 2.0$, and included 0.25 pressure scaleheights of convective overshooting from the core (Schröder, Pols & Eggleton 1997; Pols et al. 1997).

Since the accreting object is a black hole, we need to follow the change in the accretion efficiency and the change in the spin angular momentum of the black hole as its mass increases. In our calculations we assume for simplicity that the black hole is initially non-rotating. If we further assume that the efficiency, $\eta$, with which the black hole radiates is determined by the last stable particle orbit, then the black hole luminosity can be written as

$$L = \eta \dot{M}_{\rm acc} c^2, \tag{5}$$

where $\dot{M}_{\rm acc}$ is the black hole mass-accretion rate (as measured by an observer at infinity), $c$ is the speed of light and $\eta$ is approximately given by

$$\eta = 1 - \sqrt{1 - \left(\frac{M_{\rm BH}}{3M^0_{\rm BH}}\right)^2}, \tag{6}$$

for $M_{\rm BH} < \sqrt{6}M^0_{\rm BH}$. Here, $M^0_{\rm BH}$ and $M_{\rm BH}$ are the initial and the present gravitating mass–energy of the black hole, respectively (Bardeen 1970; see also King & Kolb 1999). In none of our evolutionary sequences does $M_{\rm BH}$ exceed $\sqrt{6}M^0_{\rm BH}$. Over this interval $\eta$ ranges from ~0.06–0.42 (but see footnote 2). If the black hole were born with significant rotation (as argued e.g. by LBW), all of these expressions would have to be modified accordingly.

This luminosity needs to be compared with the Eddington luminosity at which the radiation pressure force balances gravity

$$L_{\rm edd} = \frac{4\pi G M_{\rm BH} c}{\kappa}, \tag{7}$$

where $G$ is the gravitational constant and $\kappa$ is the opacity assumed to be due to pure electron scattering, i.e. $\kappa = 0.2\ (1 + X)\ {\rm cm^2\ g^{-1}}$ for a composition with hydrogen mass fraction $X$ (e.g. Kippenhahn & Weigert 1990). Equating $L_{\rm Edd}$ to $L$ in equation (5) then defines the Eddington mass-accretion rate, i.e. the maximum accretion rate at which gravity can overcome radiation pressure (for spherical accretion):

$$\dot{M}_{\rm edd} = \frac{4\pi G M_{\rm BH}}{\kappa c \eta} \tag{8}$$

$$\simeq 2.6 \times 10^{-7}\ {\rm M_\odot\ yr^{-1}} \left(\frac{M_{\rm BH}}{10\,{\rm M_\odot}}\right)\left(\frac{\eta}{0.1}\right)^{-1}\left(\frac{1+X}{1.7}\right)^{-1} \tag{9}$$

In most calculations we assume that any mass transferred in excess of the Eddington accretion rate is lost from the system, carrying with it the same specific angular momentum as the orbiting black hole, while the rest of the mass, reduced by the fractional rest mass energy lost in the radiation, is accreted by the black hole.

As the black hole accretes mass and angular momentum, its spin parameter, $a \equiv J/M^2$, increases according to

$$a = \left(\frac{2}{3}\right)^{1/2} \frac{M^0_{\rm BH}}{M_{\rm BH}} \left\{ 4 - \left[ 18 \left(\frac{M^0_{\rm BH}}{M_{\rm BH}}\right)^2 - 2 \right]^{1/2} \right\} \tag{10}$$

for $M_{\rm BH} < \sqrt{6}M^0_{\rm BH}$ (see e.g. Bardeen 1970; Thorne 1974; King & Kolb 1999).[2]

Our calculations include, as a default, orbital angular momentum losses via magnetic braking if the secondary has a convective envelope (see e.g. Verbunt & Zwaan 1981; Rappaport, Verbunt & Joss 1983), and by gravitational radiation; these affects are only important in some of the calculations with relatively low-mass donor stars in Section 3.2 (also see Section 4.4). In most cases mass transfer occurs either on a thermal time-scale or is driven by the nuclear evolution of the secondary.

### 3.2 Results of the binary evolution calculations

To illustrate the evolution of black hole binaries we first performed a sequence of models where we varied the mass of the secondary from 2 to 17 $M_\odot$. In these calculations the secondary was an initially unevolved (i.e. zero-age main-sequence) star and the black hole had an initial mass of 10 $M_\odot$. Furthermore, we assumed that the mass accretion rate on to the black hole was Eddington-limited (equation 9). Some of the main results of these sequences are shown in Figs 4 and 5 and in the top part of Table 1. All calculations were terminated either when the secondary became degenerate or when it became detached during helium core burning. In some cases, the secondary would have filled its Roche lobe again after helium core burning and ascended the asymptotic giant branch. In this relatively short-lived phase the properties of the systems would be similar to those on the ascent of the first giant branch and the orbital period would continue to increase somewhat (but typically by less than a factor of 2). In all cases with initially unevolved secondaries, the secondaries end their evolution as white dwarfs rather than in a supernova.

The main behaviour of these binary sequences is not difficult to understand; it is mainly determined by the initial mass ratio of the components ($q \equiv M_{\rm d}/M_{\rm BH}$; see e.g. Ritter 1996; Kalogera & Webbink 1996; PRP for detailed recent discussions). Generally the mass-transfer rates (bottom right panel in Fig. 4) at any point in the evolution are higher for higher initial secondary masses (mass ratios).

[2] For a maximally spinning Kerr black hole $a$ nominally approaches unity, but is probably limited by a counteracting torque owing to disc radiation swallowed by the black hole to be ~0.998 (Thorne 1974). It also limits the efficiency $\eta$ in equation (6) to ~0.30.

**Table 1.** Selected properties of binary evolution sequences.

| Initial parameters | | | Parameters for GRS 1915 | | | | | | | Final parameters | | | X-ray lifetimes | | | | |
|---|---|---|---|---|---|---|---|---|---|---|---|---|---|---|---|---|---|
| $M_{\rm d}^0$ ($M_\odot$) | $M_{\rm BH}^0$ ($M_\odot$) | $P_{\rm orb}^0$ (d) | $M_{\rm d}$ ($M_\odot$) | $M_{\rm BH}$ ($M_\odot$) | $\dot{M}$ ($M_\odot$ yr$^{-1}$) | log $T_{\rm eff}$ (K) | log $L$ ($L_\odot$) | $X_{\rm surf}$ | $a_{\rm spin}$ | $M_{\rm d}^{\rm f}$ ($M_\odot$) | $M_{\rm BH}^{\rm f}$ ($M_\odot$) | $P_{\rm orb}^{\rm f}$ (d) | $t_{\rm X-ray}$ (yr) | $t_{\rm trans}$ (yr) | $t_{[<39]}$ (yr) | $t_{[39,40]}$ (yr) | $t_{[>40]}$ (yr) |
| 2 | 10 | 0.56 | – | – | – | – | – | – | – | 0.250 | 11.63 | 14 | 3.1E+09 | 3.1E+09 | – | – | – |
| 3 | 10 | 0.62 | 0.573 | 12.25 | 4.2E−08 | 3.627 | 1.919 | 0.586 | 0.56 | 0.357 | 12.45 | 137 | 8.6E+08 | 8.3E+08 | 3.1E+07 | – | – |
| 4 | 10 | 0.68 | 0.802 | 12.95 | 1.2E−07 | 3.644 | 2.085 | 0.543 | 0.66 | 0.439 | 13.26 | 196 | 4.2E+08 | 1.6E+08 | 2.6E+08 | – | – |
| 5 | 10 | 0.73 | 0.995 | 13.66 | 2.1E−07 | 3.666 | 2.228 | 0.441 | 0.74 | 0.556 | 14.00 | 180 | 2.4E+08 | 6.0E+07 | 1.8E+08 | 1.9E+06 | – |
| 6 | 10 | 0.76 | 1.151 | 14.26 | 2.8E−07 | 3.685 | 2.354 | 0.432 | 0.79 | 0.626 | 14.70 | 194 | 1.6E+08 | 2.2E+07 | 1.3E+08 | 3.4E+06 | – |
| 7 | 10 | 0.80 | 1.321 | 14.50 | 7.5E−07 | 3.720 | 2.535 | 0.417 | 0.81 | 0.701 | 14.85 | 196 | 1.1E+08 | 5.8E+06 | 1.0E+08 | 1.9E+06 | 6.1E+04 |
| 8 | 10 | 0.83 | 1.469 | 15.00 | 1.9E−06 | 3.767 | 2.742 | 0.408 | 0.84 | 0.783 | 15.22 | 206 | 8.5E+07 | 1.9E+06 | 8.2E+07 | 4.3E+05 | 8.3E+05 |
| 9 | 10 | 0.86 | 1.599 | 15.54 | 2.8E−06 | 3.805 | 2.923 | 0.399 | 0.87 | 0.886 | 15.69 | 186 | 6.9E+07 | 1.2E+06 | 6.6E+07 | 1.3E+06 | 7.4E+05 |
| 10 | 10 | 0.88 | 1.708 | 16.05 | 4.0E−06 | 3.836 | 3.069 | 0.392 | 0.90 | 0.989 | 16.16 | 161 | 5.8E+07 | 8.7E+05 | 5.3E+07 | 3.3E+06 | 6.3E+05 |
| 11 | 10 | 0.90 | 1.798 | 16.41 | 5.0E−06 | 3.863 | 3.199 | 0.381 | 0.91 | 1.085 | 16.49 | 147 | 5.0E+07 | 6.3E+05 | 4.4E+07 | 5.4E+06 | 5.5E+05 |
| 12 | 10 | 0.92 | 1.877 | 16.63 | 5.9E−06 | 3.887 | 3.305 | 0.373 | 0.92 | 1.171 | 16.69 | 134 | 4.5E+07 | 6.4E+05 | 2.7E+07 | 1.7E+07 | 4.1E+05 |
| 13 | 10 | 0.94 | 1.939 | 16.77 | 6.8E−06 | 3.905 | 3.381 | 0.368 | 0.93 | 1.236 | 16.82 | 124 | 4.1E+07 | 5.3E+05 | 3.7E+06 | 3.7E+07 | 4.1E+05 |
| 15 | 10 | 0.97 | 1.959 | 16.83 | 7.4E−06 | 3.915 | 3.444 | 0.354 | 0.93 | 1.286 | 16.88 | 116 | 3.9E+07 | 3.8E+05 | 2.3E+06 | 3.5E+07 | 5.5E+05 |
| 17 | 10 | 1.00 | 1.924 | 16.56 | 7.0E−06 | 3.905 | 3.374 | 0.363 | 0.92 | 1.229 | 16.61 | 122 | 4.1E+07 | 4.1E+05 | 3.4E+06 | 3.5E+07 | 1.8E+06 |
| Evolved sequences | | | | | | | | | | | | | | | | | |
| 2 | 10 | 4.74 | 0.944 | 10.99 | 9.5E−08 | 3.629 | 2.049 | 0.672 | 0.30 | 0.535 | 11.37 | 162 | 1.8E+07 | 1.0E+07 | 7.1E+06 | – | – |
| 8 | 10 | 1.21 | 1.700 | 14.57 | 4.5E−06 | 3.844 | 3.106 | 0.363 | 0.82 | 0.990 | 14.68 | 162 | 4.0E+07 | 1.5E+06 | 3.7E+07 | 1.3E+06 | 6.1E+05 |
| 8 | 10 | 1.86 | 2.015 | 13.77 | 9.8E−06 | 3.923 | 3.463 | 0.288 | 0.75 | 1.186 | 13.84 | 152 | 1.7E+07 | 7.2E+05 | 6.2E+06 | 9.6E+06 | 5.0E+05 |
| 8 | 10 | 3.26 | 2.634 | 11.00 | 3.7E−06 | 3.936 | 3.593 | 0.528 | 0.31 | 1.564 | 11.12 | 138 | 4.3E+06 | 5.6E+05 | 1.5E+06 | 1.3E+06 | 9.6E+05 |
| 8 | 10 | 5.26 | 3.268 | 10.01 | 2.6E−04 | 3.850 | 3.315 | 0.700 | 0.00 | 1.963 | 10.05 | 131 | 1.2E+05 | 1.2E+04 | 2.8E+02 | 7.3E+03 | 9.7E+04 |
| Non-Eddington limited sequences | | | | | | | | | | | | | | | | | |
| 8 | 10 | 0.83 | 1.162 | 16.13 | 1.3E−06 | 3.762 | 2.672 | 0.331 | 0.90 | 0.729 | 16.50 | 106 | 9.1E+07 | 2.6E+06 | 8.7E+07 | 5.1E+05 | 8.9E+05 |
| 15 | 10 | 0.97 | 1.383 | 21.39 | 3.3E−06 | 3.941 | 3.442 | 0.238 | 1.00 | 1.163 | 21.55 | 48 | 4.2E+07 | 6.2E+05 | 1.4E+06 | 3.9E+07 | 5.4E+05 |

*Note.*

Initial Parameters – $M_{\rm d}^0$, $M_{\rm BH}^0$: initial masses of the secondary and the black hole, $P_{\rm orb}^0$: initial orbital period.

Parameters for GRS 1915 (i.e. at $P_{\rm orb} = 33.5$d) – $M_{\rm d}$, $M_{\rm BH}$: masses of the secondary (the donor star) and the black hole, $\dot{M}$: mass-transfer rate, $T_{\rm eff}$, $L$, $X_{\rm surf}$: effective temperature, luminosity, surface hydrogen mass fraction of the secondary, $a_{\rm spin}$: black hole spin parameter.

Final parameters of the sequences – $M_{\rm d}^{\rm f}$, $M_{\rm BH}^{\rm f}$: final masses of the secondary and the black hole, $P_{\rm orb}^{\rm f}$: final orbital period.

X-ray lifetimes – $t_{\rm X-ray}$: total lifetime of all X-ray phases, $t_{\rm trans}$: overall lifetime of transient X-ray phases, $t_{[<39]}$, $t_{[39,40]}$, $t_{[>40]}$: lifetimes of steady X-ray phases with potential X-ray luminosities with $L_{\rm X} < 10^{39}$ erg s$^{-1}$, $10^{39}$ erg s$^{-1}$ $< L_{\rm X} < 10^{40}$ and $L_{\rm X} > 10^{40}$ erg s$^{-1}$, respectively.

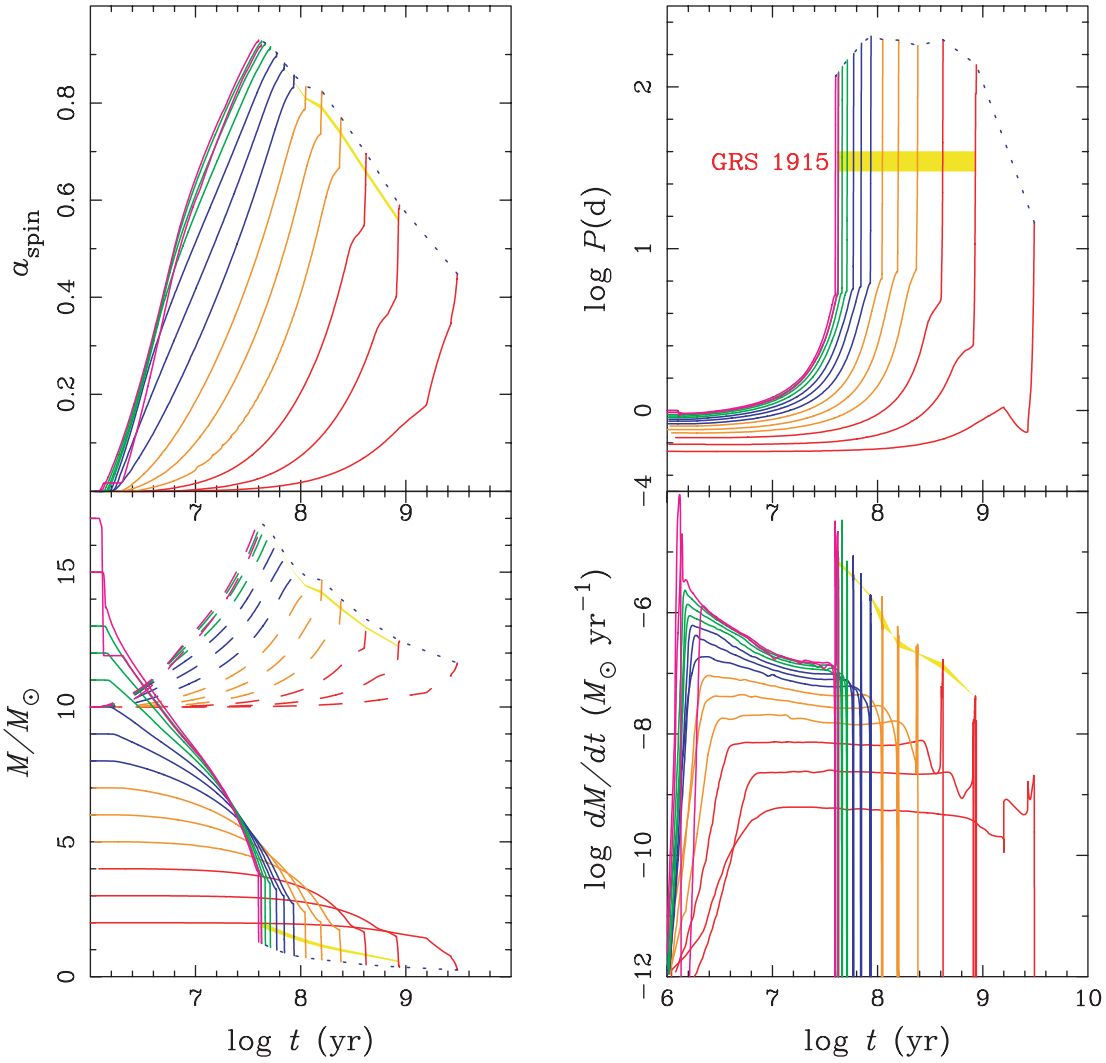


**Figure 4.** Selected properties of the evolutionary sequences for black hole binaries with initially unevolved secondaries of 2 to 17 $M_\odot$ (see Table 1) as a function of time since the beginning of mass transfer (with arbitrary offset). The initial mass of the black hole is 10 $M_\odot$ in all sequences. Top left panel: black hole spin parameter ($J/M^2$); top right panel: orbital period; bottom left panel: black hole mass (dashed curves) and secondary mass (solid curves); bottom right panel: mass-transfer rate. The shaded regions in each panel indicate the period range of 30 to 40 d (similar to the orbital period of GRS 1915+105 with $P_{\rm orb} = 33.5$ d).

For relatively low-mass secondaries, the secondaries always remain close to thermal equilibrium and mass transfer is entirely driven by the nuclear evolution of the secondary. The mass-transfer rate tends to dip near the end of the secondary's main-sequence phase, where the secondary may even become detached temporarily, and then increases sharply as the secondary ascends the giant branch where the evolution is determined by the rate at which the hydrogen-burning shell advances through the star. For the more massive secondaries ($q > 1$), the mass-transfer time-scale becomes shorter than the thermal time-scale of the secondary and mass transfer occurs initially on the thermal time-scale of the secondary's envelope. For the most massive secondaries this leads to a sharp initial spike in the mass-transfer rate, reaching a peak of $\dot{M} \sim 10^{-4}\,{\rm M}_\odot\,{\rm yr}^{-1}$. Note that after this initial high mass-transfer rate, the evolution of all sequences with $M \gtrsim 12\,{\rm M}_\odot$ becomes essentially uniform and independent of the initial mass of the secondary.[3]

For secondaries with initial masses larger than ~20 $M_\odot$ (not shown in the figures; but see Section 4.3), the initial mass-transfer rate would become so high that mass transfer would become unstable (i.e. experience a delayed dynamical instability; Hjellming & Webbink 1987; PRP) and the secondary would then be likely to engulf the black hole leading to a second common-envelope phase and the spiral-in of the black hole in this envelope.[4] The further

[3] This is only true for secondaries that are initially relatively unevolved which after the initial high mass-transfer phase behave like lower mass secondaries. If the secondaries have already established a very non-uniform chemical composition profile, the subsequent evolution can be drastically altered (see e.g. Podsiadlowski & Rappaport 2000).

[4] In the calculation with an initially unevolved 20-$M_\odot$ star, the secondary never overfilled its Roche lobe by more than 14 per cent (for a short period of time). It is not entirely clear whether this necessarily leads to a spiral-in phase, in particular for stars with radiative envelopes (Podsiadlowski 2001). If it does not, and the system survives the initial phase of high mass transfer, the secondary becomes detached after it has reestablished thermal equilibrium (similar to fig. 7 in PRP); but the secondary now has a mass of only 4 $M_\odot$ and the subsequent evolution will mimic the evolution of a system with a

evolution in this case is presently rather uncertain; the black hole will most likely settle at the centre of the secondary destroying its core or merging with it. The ultimate product will be a black hole with a possibly much larger mass than the initial mass if it is able to accrete a substantial fraction of the secondary (e.g. if accretion occurs in the supercritical regime where radiation can be trapped in the flow; Houck & Chevalier 1991; Chevalier 1993). In addition, the black hole may be surrounded by planet-mass objects or one or more low-mass stars that are likely to form by gravitational instabilities in the centrifugally supported disc left over from the collapsing envelope of the secondary (for more details of such a scenario see Podsiadlowski et al. 1995). If the black hole is indeed orbited by a low-mass stellar companion, the system may later appear again as an X-ray binary, but would now be classified as a low-mass black hole binary. Note, however, that the secondary should be chemically anomalous for its mass since it is likely to contain matter that underwent nuclear processing in a massive star (i.e. show evidence for CNO processing).

Returning to Fig. 4, the left bottom panel shows that the black hole mass (dashed curves) can increase substantially in these sequences, by up to $\sim$7 $M_\odot$ (also see Table 1), even though we assumed that mass accretion on to the black hole was Eddington-limited. Most of this accretion takes place when the secondary is still burning hydrogen in the core since this phase lasts much longer than the subsequent giant phase and since the mass-transfer rates on the giant branch are generally much higher, often significantly super-Eddington. This has the consequence that a larger fraction of the transferred mass is lost from the system.

Our finding that the black hole can accrete a fairly significant amount of mass is in apparent conflict with the results of a related study by King & Kolb (1999) who found a much more moderate possible increase of the black hole mass ($\lesssim$ 2.5 $M_\odot$) by estimating the maximum amount that can be accreted as the product of the Eddington accretion rate and the evolutionary time-scale of the secondary. The differences in these results can be attributed to two factors. First King & Kolb (1999) used a characteristic value for the Eddington accretion rate ($10^{-7}$ $M_\odot$ yr$^{-1}$ for a 10 $M_\odot$ black hole) that is substantially lower (up to a factor of $\sim$4) than the value given by equation (9) in the early phase of the evolution when the black hole radiation efficiency is low ($\eta \simeq 0.06$). A second factor is that, in particular for the more massive secondaries, the characteristic evolutionary time-scale increases as the mass of the secondary decreases and as the secondary behaves like a less massive star. This increases the evolutionary time-scale by between a factor of $\sim$2.5 for the least massive secondaries to $\sim$4 for the more massive secondaries in our calculations (a factor of 100 in the 20-$M_\odot$ calculation).

However, all of the calculations presented so far assume that the secondary is initially unevolved. As the results in Section 2 show, it is much more likely that the secondary was at least somewhat evolved at the beginning of mass transfer. Since this shortens the remaining evolutionary time in the hydrogen core-burning phase, it reduces the amount of matter that can be accreted by the black hole. To illustrate this we have performed four evolutionary sequences for a secondary with an initial mass of 8 $M_\odot$ at different evolutionary stages (see 'Evolved Sequences' in Table 1). In these calculations the secondaries had a hydrogen mass fraction in the core at the beginning of mass transfer of $X = 0.50, 0.30, 0.10$ in the first three sequences, respectively, while in the fourth sequence the secondary already had developed a hydrogen-exhausted core of 0.7 $M_\odot$ (i.e. experienced so-called early case B mass transfer). As expected, the final black hole mass decreases systematically from 15.2 $M_\odot$ for the initially unevolved secondary to only 11.1 $M_\odot$ for the secondary near the end of the main-sequence phase. In the calculation where mass transfer starts after the main-sequence phase of the secondary, the black hole accretes only $\sim$0.05 $M_\odot$. Nevertheless, even for an initially moderately evolved secondary, the black hole mass can still increase quite substantially (by $\sim$4 $M_\odot$).

As the black hole accretes matter from the last stable orbit, it also accretes angular momentum and is spun up in the process. The top left panel in Fig. 4 shows the time evolution of the black hole spin parameter $a$ (equation 10). Even if the black hole was completely non-rotating initially (as we assumed in our sequences) and the accretion rate is Eddington-limited, the black hole can be spun up substantially to a spin parameter $a \sim 0.9$, where for a maximally rotating Kerr black hole $a = 0.998$ (Thorne 1974).

In Fig. 5 we show the distribution (indicated by shading) of the spin parameter (top panels) and the *potential* X-ray luminosity, defined below, (bottom panels) for selected evolutionary sequences of the secondary both in the orbital period–secondary mass plane (left panels), and in the Hertzsprung–Russell (HR) diagram (right panels). In these figures, the solid curves represent selected evolutionary sequences with initially unevolved secondaries (as indicated). Note in particular how the evolutionary tracks for the most massive secondaries all converge and how the effective temperature in the red giant phase increases systematically with initial secondary mass. The latter is in part caused by the much lower hydrogen abundance in the envelope of the initially more massive secondaries (see Table 1). The dashed curves in the panels indicate the black hole mass (from 10 to 16 $M_\odot$).

In the bottom panels of Fig. 5 we have defined a '*potential* X-ray luminosity' as the accretion luminosity from the black hole assuming that all the matter that is transferred from the secondary is accreted by the black hole radiating at the appropriate efficiency $\eta$ (equation 6), i.e. assuming that accretion is not Eddington-limited (see e.g. Begelman 2002). Because of the high mass-transfer rate, in particular for the more massive systems, this *potential* X-ray luminosity can be as high $\sim 10^{41}$ erg s$^{-1}$ and systems can spend a large fraction of their X-ray-active lifetime at these high mass-transfer rates (see the X-ray lifetimes in Table 1 and the further discussion in Section 4.2). Fig. 5 also shows where systems would be expected to be black hole transients (light shading). To decide whether a system exhibits transient behaviour, we utilized an expression very similar to equation (A5) of Vrtilek et al. (1990) for determining the outer disc temperature at $r_d$. If $T_{\rm e}\,(r_{\rm d})$ is found to be $\gtrsim$6500 K, we take the disc to be ionized, and therefore *not* subject to the standard thermal ionization disc instability (Cannizzo & Wheeler 1984; van Paradijs 1996; King, Kolb & Szuskiewicz 1997; Lasota 2002). As expected from the behaviour of the mass-transfer rates (Fig. 4), systems with relatively low-mass secondaries tend to be transient systems, and the *potential* X-ray luminosities increase systematically with initial secondary mass.

When interpreting these results, several caveats are in order. The actual binary evolution calculations leading to the results discussed above assumed that any mass transferred in excess of the Eddington rate was lost from the system; this, in turn, somewhat affects the evolution of the orbit and the mass-transfer rate itself. In order to estimate how sensitive our results for the *potential* luminosity are to

4-$M_\odot$ secondary. It starts to fill its Roche lobe shortly after the hydrogen core-burning phase (i.e. experience early case B mass transfer) and has parameters at an orbital period of 33.5 d consistent with those of GRS 1915+105 (see Section 4.1).

the assumption of Eddington-limited accretion, we performed two sequences where we assumed that accretion on to the black hole was not Eddington-limited for secondaries with an initial mass of 8 and 15 $M_\odot$, respectively (see 'non-Eddington limited sequences' in Table 1). The 8-$M_\odot$ sequence is only moderately affected since the mass-transfer rate is sub-Eddington for most of the evolution, while in the 15-$M_\odot$ sequence the black hole mass grows significantly larger, as expected, than in the Eddington-limited case. But even for the more massive secondary, the mass-transfer rates are typically within a factor of 2 at the same orbital period for the Eddington-limited and the non-limited case. We therefore conclude that the inferred *potential* X-ray luminosities are correct as computed to within a factor of a few. Since the Eddington luminosity in our systems with the highest mass black holes ($\sim$17 $M_\odot$) is $4 \times 10^{39}$ erg s$^{-1}$, an observed X-ray luminosity as high as $10^{40}$ erg s$^{-1}$ would require only a modest super-Eddington mass accretion rate of a factor of a few $\dot{M}_{\rm edd}$. Even for systems with *potential* X-ray luminosities as high as $10^{41}$ erg s$^{-1}$, mass accretion has to exceed the Eddington accretion rate by typically less than a factor $\sim$20. These super-Eddington accretion rates may be significantly reduced if beaming of the X-ray flux is important in these systems (King et al. 2001). Begelman (2002) has recently reexamined the problem of super-Eddington accretion and concluded that in radiation-pressure-dominated accretion discs, super-Eddington accretion rates of a factor of 10 to 100 can be achieved, owing to the existence of a photon-bubble instability in magnetically constrained plasmas. In this context, it is worth pointing out that a number of X-ray binaries containing neutron stars are known to radiate substantially above the Eddington limit (SMC X-1, Levine et al. 1993; LMC X-4, Levine et al. 1991) by factors of up to $\sim$5. It is believed that this is a consequence of the fact that the accretion on to the poles of the neutron star is funnelled through a strong magnetic field, a process that is not directly applicable to black hole systems. Nevertheless, it demonstrates that super-Eddington X-ray binaries exist in nature (also see Section 4.1).

It is also worth pointing out that the mass-transfer rates obtained from our calculations are secular mass-transfer rates, i.e. represent an average over time-scales much longer than the lifetime of X-ray astronomy. It is quite plausible that the mass-transfer rates fluctuate substantially about the secular mean even in systems that are not considered 'transients' according to the disc-instability model. GRS 1915+105 may present an example for this. It became an X-ray source in 1992 (Castro-Tirado, Brandt & Lund 1992) and has been a relatively steady source ever since (Sazonov et al. 1994; Greiner, Morgan & Remillard 1997; http://xte.mit.edu). Its behaviour is very different from the normal behaviour of soft X-ray transients and the system could probably be better classified as a semipersistent source.

## 4 APPLICATIONS

### 4.1 GRS 1915+105

One of the best-studied black hole binaries in the Galaxy is the microquasar GRS 1915+105 (see e.g. Castro-Tirado et al. 1992; Greiner, Morgan & Remillard 1996; Mirabel & Rodríguez 1994). Greiner, Cuby & McCaughrean (2001) recently determined the orbital period of the system as $33.5 \pm 1.5$d and obtained the black hole mass function ($f(M) = 9.5 \pm 3.0$ $M_\odot$). Based on their analysis, they find a black hole mass of $14 \pm 4$ $M_\odot$, substantially more massive than the masses inferred for the majority of black hole transients (see e.g. table 1 in LBW and references therein; Orosz et al. 2002). In Figs 4 and 5, we indicated the period range of 30 to 40 d, i.e. close to the period of GRS 1915+105, in all panels and in Table 1 we give some of the key system parameters of all evolutionary sequences at an orbital period of 33.5 d. The sequence with an initially unevolved secondary of 2 $M_\odot$ never reaches an orbital period of 33.5 d. The reason is that in this case (unlike the other cases), magnetic braking becomes important, indeed the dominant mass-transfer driving mechanism, at the end of the donor's main-sequence phase; this causes a peak in $\dot{M}$ and a temporary shrinking of the orbit (see Fig. 4). We therefore added another sequence with an initial secondary of 2 $M_\odot$ which has already evolved off the main sequence at the beginning of mass transfer (i.e. experienced case B mass transfer). Since the evolution of low-mass giants is entirely determined by the evolution of the core mass (and not the total mass), this sequence can also be considered representative for systems with low-mass secondaries in general (as assumed e.g. by Belczynski & Bulik 2002; Vilhu 2002 in their modelling of GRS 1915+105).

As Table 1 shows, the masses of both components and the mass-transfer rate at an orbital period of 33.5 d increase systematically with the mass of the secondary, reaching a maximum for an initial secondary of $\sim$15 $M_\odot$. The same applies to the effective temperature and the luminosity. Greiner et al. (2001) have estimated the spectral type of the secondary as K-M III. Since a K0 III star has an effective temperature of $\sim$4800 K (e.g. Straižys & Kuriliene 1981), we can use this as an additional constraint to limit the possible evolutionary histories of GRS 1915+105. Inspection of Table 1 then suggests that acceptable models for GRS 1915+105 can have initial secondary masses as high as 6 $M_\odot$. Indeed the model parameters for GRS 1915+105 in the 6 $M_\odot$ sequence are very close to the system parameters deduced by Greiner et al. (2001; $M_{\rm BH} \sim 14$ $M_\odot$, $M_{\rm d} \sim 1.2$ $M_\odot$), for an assumed system inclination angle of $\sim$70°, as determined from the orientation of the jets (Mirabel & Rodríguez 1994). We note that in principle one could use the 'transient' nature of GRS 1915+105 to further constrain the evolutionary past of the system. However, considering the unusual X-ray behaviour of GRS 1915+105, which is very different from the predictions of the simple disc-instability model, this is probably not advisable (see the discussion at the end of Section 3.2).

Our calculations have several important implications for GRS 1915+105. First, they show that the mass of the black hole may have increased significantly, by up to $\sim$4 $M_\odot$, even if the mass accretion rate is, on average, Eddington-limited (also see LBW who obtained a similar estimate). Hence the present mass of the black hole is not a good indicator of the initial black hole mass, and any analysis of the implications of observed black hole masses for the evolution of the black hole progenitor has to take this into account. We have calculated some additional evolutionary sequences starting with a lower black hole mass of 7 $M_\odot$ (similar to the masses found in other black hole binaries) and obtained acceptable models for GRS 1915+105 with black hole masses as high as 11 $M_\odot$.

Secondly, since the black hole may have accreted a substantial amount of matter, it may also have been spun up significantly and may have acquired a spin parameter as high as $a \sim 0.8$ (assuming an initially non-rotating black hole). This may be important for modelling the jets and the emission from the inner parts of the accretion disc (e.g. Zhang, Cui & Chen 1997; Makishima et al. 2000).

Thirdly, the secular mass-transfer rate can be as high as $\sim 3 \times 10^{-7}$ $M_\odot$ yr$^{-1}$, implying an X-ray luminosity as high as $\sim 2 \times 10^{39}$ erg s$^{-1}$. This is a factor of a few lower than the peak X-ray luminosity of $7 \times 10^{39}$ erg s$^{-1}$, determined for GRS 1915+105 by

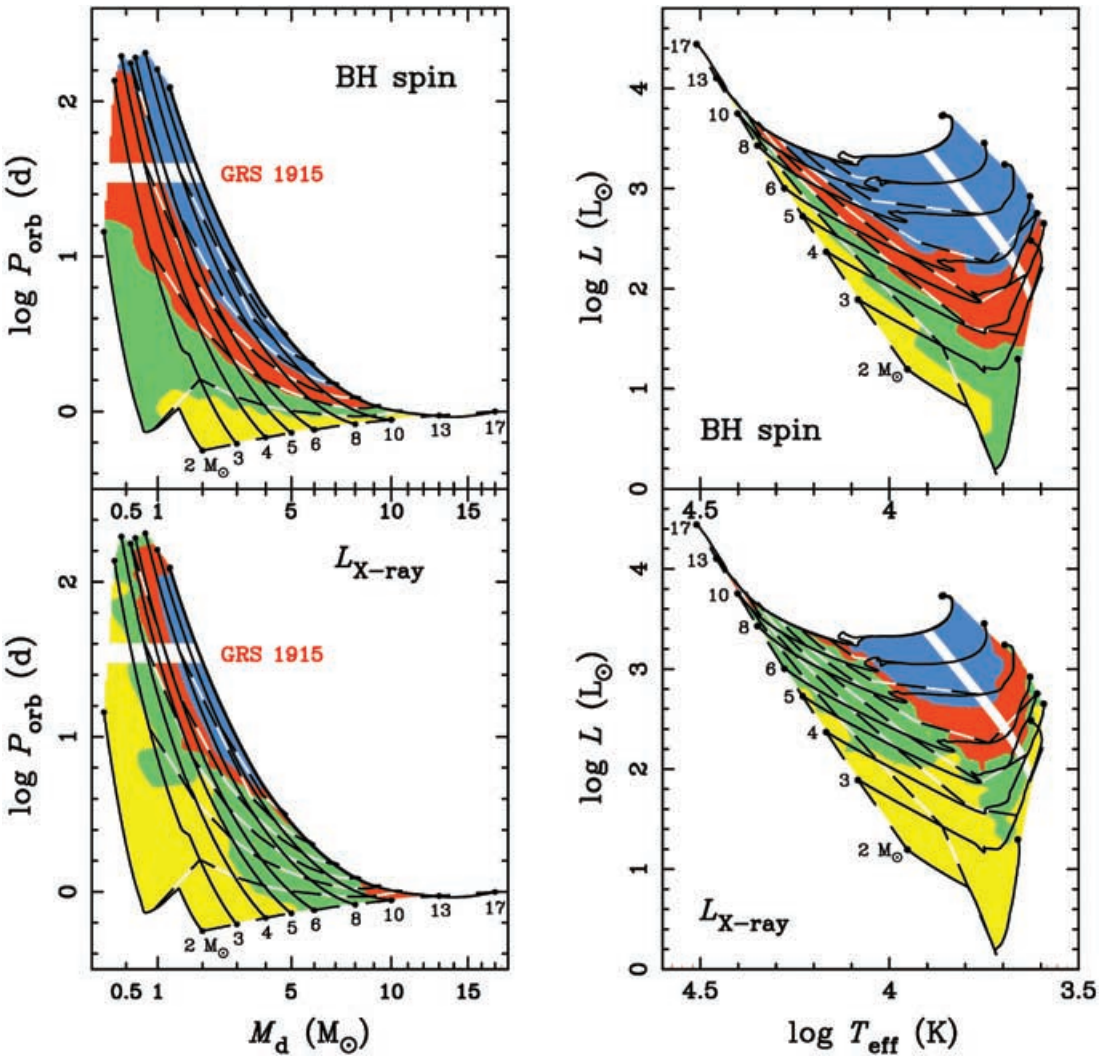


**Figure 5.** Shaded contours of black hole spin parameter ($J/M^2$) (top panels) and *potential* X-ray luminosity (bottom panels) (i.e. the luminosity assuming that all the mass transferred is accreted by the black hole) in the $P_{orb}$–$M_d$ (orbital period–secondary mass) plane (left panels) and in the HR diagram (right panels). Shading for the black hole spin (from light to dark): 0–0.25; 0.25–0.50; 0.50–0.75; 0.75–1.00. Shading for the *potential* X-ray luminosity (from light to dark): transient X-ray sources; steady sources with $L_X < 10^{39}$ erg s$^{-1}$); $10^{39} < L_X < 10^{40}$ erg s$^{-1}$; $L_X > 10^{40}$ erg s$^{-1}$. The solid curves show the evolutionary tracks for the initially unevolved secondaries in Table 1 and Fig. 4 with the initial masses as indicated. The dashed curves are contours of constant black hole mass (10, 11, 12, 13, 14, 15, 16 $M_\odot$ from left to right [right panels], bottom to top [left panels]). The white strips indicate the position of systems with orbital periods between 30 and 40 d, i.e. have an orbital period similar to GRS 1915+105.

Greiner et al. (1996). This implies that only a moderate amount of super-Eddington accretion is required to explain the observed peak luminosity in our models to explain the observed luminosity.

Fourthly, our models predict that the surface abundance of the secondary should be substantially enhanced in helium and could show CNO abundance ratios that are close to the equilibrium ratios for the CNO cycles (in particular for the more massive secondaries). This provides a potentially powerful test that may help to constrain further the nature and the initial mass of the secondary.

### 4.2 Ultraluminous X-ray sources

Ultraluminous X-ray sources (ULX) are luminous X-ray sources outside the nuclei of external galaxies, typically defined to have an X-ray luminosity larger than $10^{39}$ erg s$^{-1}$. They were originally discovered by *Einstein* (Fabbiano 1989) and have been found in large numbers by *ROSAT* and most recently *Chandra* (Colbert & Mushotzky 1999; Roberts & Warwick 2000; Colbert & Ptak 2002; Lira, Johnson & Lawrence 2002; Jeltema et al. 2002). While the physical nature of these sources has remained unclear, and indeed they probably form a heterogeneous class of systems (Kilgard et al. 2002; Roberts et al. 2002), a plausible scenario is that they constitute the luminous tail of the stellar-mass black hole binary distribution (for recent discussions see Colbert & Mushotzky 1999; King et al. 2001; King 2002; Roberts et al. 2002). With an inferred peak X-ray luminosity of $7 \times 10^{39}$ erg s$^{-1}$ (Greiner et al. 1996), GRS 1915+105 certainly classifies as a typical ULX (King et al. 2001; Mirabel & Rodríguez 1999). The connection of ULXs with 'normal' Galactic black hole binaries has been strengthened by the determination of the black hole mass in GRS 1915+105 (Greiner et al. 2001), which proved that ULXs may contain typical stellar-mass black holes rather than a previously unknown class of intermediate-mass black holes of $10^2$–$10^4$ $M_\odot$ (as suggested by Colbert & Mushotzky 1999).

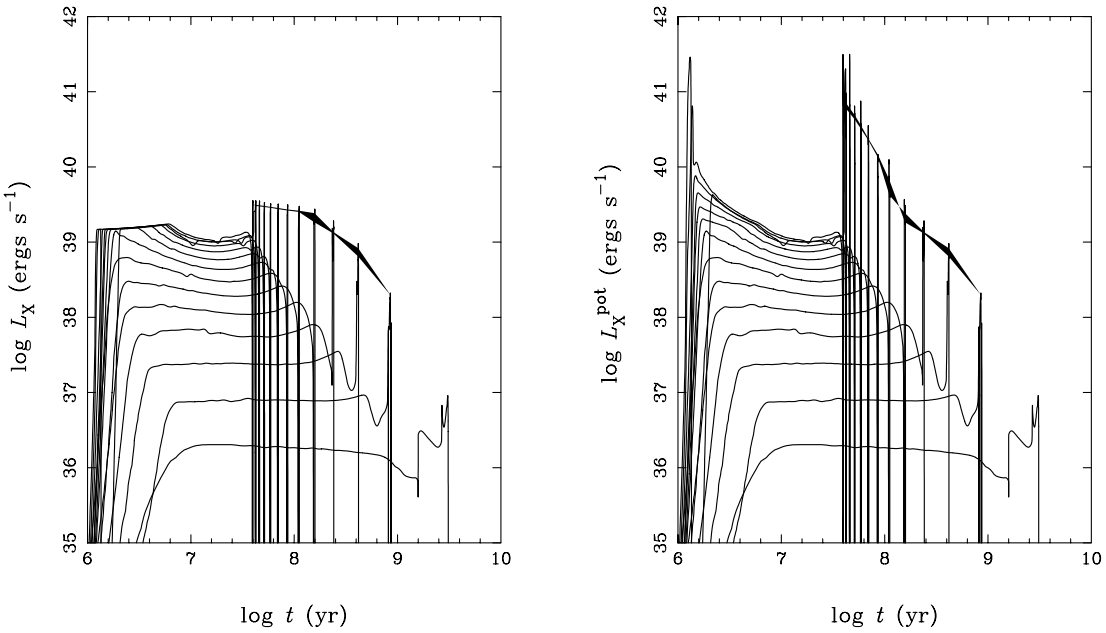


**Figure 6.** X-ray luminosity, assuming Eddington-limited accretion, (left) and *potential* X-ray luminosity, assuming non-Eddington-limited accretion, (right) for the binary sequences with unevolved secondaries (see Fig. 4) as a function of time since the beginning of mass transfer. The shaded regions in each panel indicate the period range of 30 to 40 d (similar to the orbital period of GRS 1915+105 with $P_{\rm orb} = 33.5$ d). This figure is available in colour in the online version of the journal on *Synergy*.

The calculations presented in this paper strongly support the connection of ULXs with black hole binaries, in particular those with intermediate-/high-mass secondaries. Fig. 6 shows both the X-ray luminosity (assuming Eddington-limited accretion) and the *potential* X-ray luminosity (assuming non-Eddington-limited accretion) of the binary sequences. While the Eddington-limited luminosity reaches a maximum of $\sim 4 \times 10^{39}$ erg s$^{-1}$, the *potential* X-ray luminosity can be as high as $\sim 3 \times 10^{41}$ erg s$^{-1}$ and could be even higher if the mass-transfer rate is variable (consistent with observations; see e.g. Lira et al. 2002 and the discussion at the end of Section 3.2). Our calculations therefore show that the mass-transfer rates in these sequences are high enough to provide a potential power source for ULXs. It requires only that the majority of ULXs have to radiate at a moderately super-Eddington luminosity, as is actually observed in GRS 1915+105. Even for the most luminous observed ULXs, the luminosity has to exceed the Eddington luminosity by a factor of $\lesssim$20, which may not pose a serious problem in radiation-pressure-dominated magnetic discs (Begelman 2002). This factor may be further reduced significantly if the radiation is beamed (King et al. 2001). Fig. 5 shows where the most luminous systems (dark shading) are expected to lie in the HR diagram of the secondary and in the orbital period–secondary mass plane. They indicate that black hole binaries are most likely to appear as ULXs when they are giants or supergiants where mass transfer is driven by the nuclear evolution of the secondary, a phase that can last up to several $10^7$ yr (also see Fig. 6 and Table 1).

If ULXs in external galaxies are associated with intermediate-/high-mass black hole binaries, they should be preferentially found near star-forming regions. Indeed there is some evidence that many ULXs are found in regions of active star formation, starburst galaxies and interacting galaxies (Lira et al. 2002; Roberts et al. 2002; Terashima & Wilson 2002; Zezas et al. 2002). On the other hand, Colbert & Ptak (2002) found that the number of ULXs per galaxy is actually higher in elliptical than in non-elliptical galaxies and that there is a population of ULXs in the halos of elliptical galaxies, where recent star formation is not expected to have occurred. This may suggest that our models are not directly applicable to these ULXs, unless these galaxies experienced some relatively recent star formation (e.g. as a result of some previously unrecognized merger activity). King (2002) has recently proposed that there are two classes of ULXs: relatively massive systems associated with young stellar populations and low-mass systems found in old populations. Indeed there is some evidence that a large fraction of ULXs in elliptical galaxies are located in globular clusters (see e.g. Angelini, Loewenstein & Mushotzky 2001; Kundu, Maccarone & Zepf 2002; White, Sarazin & Kulkarni 2002; Jeltema et al. 2002). These could be relatively long-period systems with giant donors (at the current epoch) that formed dynamically in the dense cluster cores by processes not considered in the present study.

In principle we could combine the results of our evolutionary calculations with the BPS model in Section 2 and predict the properties of black hole binaries in a typical galaxy (e.g. the X-ray luminosity function; see Roberts & Warwick 2000). However, there are a large number of uncertainties involved, including the histories of stellar and globular cluster formation in galaxies (especially for ellipticals), as well as those associated with the modelling of the evolution that leads to the formation of a black hole binary and the problem of how to relate secular mass-transfer rates to observable X-ray luminosities. In view of these, we cannot yet hope to compute reliably a population synthesis of black hole binaries in external galaxies, and therefore little of substance is to be gained from such an exercise. However, putting aside some of these issues, e.g. the question of super-Eddington accretion, and taking the *potential* X-ray luminosity as a measure of the X-ray luminosity, one can obtain a qualitative idea of the relative number of systems by considering how much time systems spend at various mass transfer rates.

In Table 1 we list the X-ray lifetimes for transient phases and various ranges of *potential* X-ray luminosity in our binary sequences. Systems with relatively low-mass secondaries are expected to be transients for most of their evolution, while the systems with the

most massive secondaries spend a large fraction of their X-ray lifetimes as ULXs. Considering that our standard BPS model predicts a fairly uniform distribution of secondary masses, at least above some characteristic minimum mass (see Fig. 2), and taking the 11-$M_\odot$ donor sequence as typical, we then estimate that some 10 per cent of black hole binaries should be ULXs, and some 10 per cent of these have *potential* X-ray luminosities above $10^{40}$ erg $s^{-1}$. This would appear to be in qualitative agreement with the luminosity distribution of Roberts & Warwick (2000) who found that the number of sources in each decade of X-ray luminosity decreases according to $L_X^{-0.8}$. Estimates of the absolute numbers of such binaries residing in a typical Milky Way type galaxy can be made by taking the formation rates from Fig. 3 for black hole binaries with different initial donor masses and multiplying them by the various lifetimes given in Table 1. Such an exercise shows that for conventional values of the $\lambda$ parameter near $\sim$0.5 the predicted numbers of ULXs is substantially in excess of what is observed. However, for values of $\lambda$ closer to more realistic values of $\sim$0.1, the computed numbers of ULXs is quite reasonable.

Finally we note a piece of observational evidence that suggests the high luminosities inferred for some of the ULXs on the assumption of roughly isotropic emission are, in fact, correct. Pakull & Mirioni (2002) have studied very large ($\sim$300 pc) and luminous ionization nebulae surrounding about a dozen ULXs. They use the emission lines from these nebulae as an interstellar medium calorimeter to infer the long-term (e.g. $\sim 10^4$ yr; see e.g. Chiang & Rappaport 1996) mean X-ray luminosity of the underlying ULXs. From the structure of the ionization nebulae they can also rule out in some cases any extreme beaming of the radiation. The results of this study seem to point to good agreement between the X-ray luminosity determined from *Chandra* and *ROSAT* and that found indirectly from studies of the ionization nebulae.

### 4.3 Cygnus X-1

One of the most famous black hole binaries is Cyg X-1 with an orbital period of 5.6 d and a massive secondary (HDE 226868) of spectral type O9.7 Iab (Walborn 1973; Gies & Bolton 1986). It has a mass function of $0.252 \pm 0.010$ $M_\odot$ (Gies & Bolton 1982) and used to be one of the best early black hole candidates before the identification of low-mass black hole transients with much larger mass functions. However, the evolutionary state of the system has so far not been properly established; in particular it is not clear how much mass the donor star has already lost.

In Fig. 7 we present the results of a binary calculation that may represent the evolution of Cyg X-1 and which illustrates several characteristic properties of a massive black hole binary. In this model, the initial masses of the black hole and the secondary are 12 and 25 $M_\odot$, respectively, and the secondary starts to fill its Roche lobe near the end of its main-sequences phase, when its central hydrogen mass fraction has been reduced to 0.054. The orbital period at this point is 6.8 d. Unlike our previous calculations we also included a stellar wind from the secondary of $3 \times 10^{-6}$ $M_\odot$ $yr^{-1}$ (Herrero et al. 1995), taken to be constant throughout the evolution.

The general evolution is reminiscent of that of an intermediate-mass neutron star binary (see Fig. 7 in PRP and the associated discussion). After a brief turn-on phase, mass transfer occurs initially on the thermal time-scale of the envelope reaching a peak mass-transfer rate of $\sim 4 \times 10^{-3}$ $M_\odot$ $yr^{-1}$. Once the mass of the secondary has been reduced to a value comparable to the black hole, the secondary reestablishes thermal equilibrium and becomes detached. Indeed because of the continuing wind mass loss the donor shrinks significantly below its Roche lobe during this phase and the system widens. The secondary starts to expand again after it has exhausted all of the hydrogen in the core and fills its Roche lobe for a second time. In this phase, the mass-transfer rate reaches a second peak of $\sim 4 \times 10^{-4}$ $M_\odot$ $yr^{-1}$, where mass transfer is driven by the evolution of the H-burning shell. The calculation was terminated at this stage, but the secondary would ultimately become a $\sim$8 $M_\odot$ helium star, quite possibly becoming a black hole itself in the final supernova explosion.

The most interesting feature of this calculation is that the system becomes detached after the initial thermal time-scale phase because of the stellar wind from the secondary (it acts both to widen the orbit and to shrink the stellar radius). During this phase, mass transfer continues via the stellar wind. Since the secondary is close to filling its Roche lobe, such a wind may be focused towards the accreting black hole, as has been inferred from the tomographic analysis of the mass flow in Cyg X-1 by Sowers et al. (1998). In this particular calculation, the secondary has a temperature of $\sim$31 000 K at an orbital period of 5.6 d, in excellent agreement with the O9.7 spectral type of HDE 226868. It is worth noting that such a phase will generally not exist for high-mass neutron-star X-ray binaries since, because of the more extreme mass ratio in these systems, Roche-lobe overflow will generally become dynamically unstable leading to the spiral-in of the neutron star in the envelope of the massive secondary. If Cyg X-1 is in the phase described above, the model makes the firm prediction that the secondary should be significantly helium enriched and its surface composition should show strong evidence for CNO processing (in this particular model, the surface helium mass fraction is 0.55, i.e. roughly twice solar, at an orbital period of 5.6 d). Interestingly, both Herrero et al. (1995) and Canalizo et al. (1995) claim to have determined just such abundance anomalies in the secondary of Cyg X-1, which they argue cannot be accounted for by uncertainties in the atmosphere modelling.

One caveat is that this model also predicts that the mass of the secondary should at the present time be comparable to, or lower than, the mass of the black hole. This does not appear to be consistent with the analyses of Gies & Bolton (1986), using rotational velocities and assuming synchronous rotation, and Gies et al. (2002), based on an H$\alpha$ emission-line analysis. Both studies suggest that the secondary is a factor $\sim$2–3 times more massive than the black hole.

However, irrespective of whether this particular model is applicable to Cyg X-1, the calculation in Fig. 7 illustrates that it is generally more likely to observe a high-mass black hole X-ray binary in the relatively long-lived wind mass-transfer phase following the initial thermal time-scale phase which only lasts a few $10^4$ yr. In this example, the wind phase lasts a few $10^5$ yr, but it could last as long as a few $10^6$ yr if the secondary were initially less evolved.[5] This means that any secondary observed in a massive black hole binary is likely to have already lost a significant fraction of its mass and that it is generally not valid to deduce the mass of a secondary based on its spectral type alone, as is frequently done in the literature.

### 4.4 Low-mass black hole binaries

In the binary population synthesis study discussed in Section 2 and the detailed binary evolution calculations presented in Section 3

[5] Note that, if the initial mass ratio were more extreme, the initial mass transfer would become dynamically unstable, as in the case of massive neutron-star binaries, and the black hole would spiral into the massive star. In this case, there would be no subsequent wind mass-transfer phase.

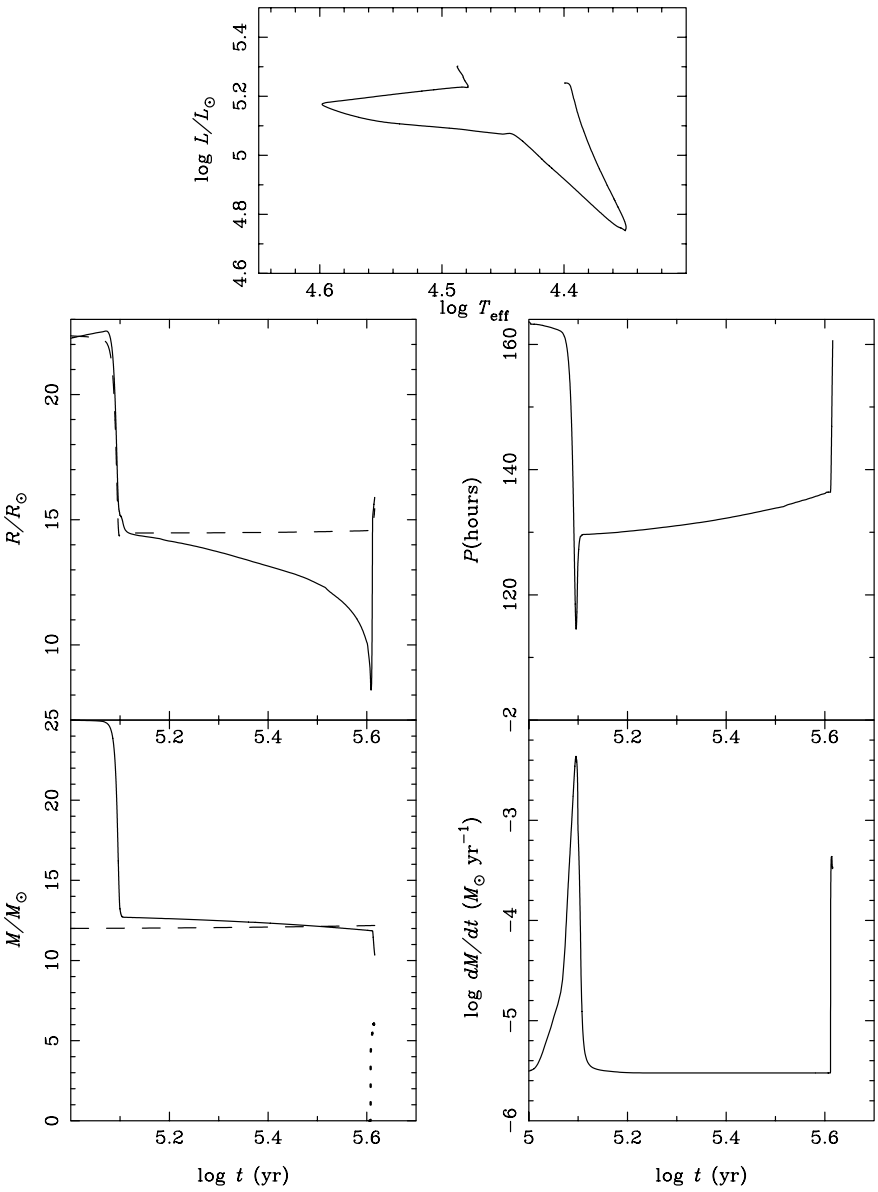


**Figure 7.** Evolutionary model for Cyg X-1. HR diagram (top panel) and key binary parameters as a function of time since the beginning of mass transfer (with arbitrary offset). Middle left: radius of the secondary (solid curve) and Roche-lobe radius (dashed curve). Middle right: orbital period. Bottom left: mass of the secondary (solid curve), the black hole (dashed curve) and the mass of the hydrogen-exhausted core (dotted curve). Bottom right: mass-loss rate of the secondary. The secondary initially has a mass of 25 $M_\odot$ and has already exhausted most of its hydrogen in the core (it has a core hydrogen mass fraction $X = 0.054$). The initial mass of the black hole is 12 $M_\odot$ and barely changes during the evolution. The calculation includes a constant stellar wind from the secondary with a mass-loss rate of $3 \times 10^{-6}$ $M_\odot$ yr$^{-1}$, consistent with the present observations of the secondary in Cyg X-1. The black hole accretion rate is always limited by the Eddington accretion rate.

hardly any black hole binaries were formed with low-mass donors, and all the systems that were evolved in detail developed into wide, rather than close binaries. Thus, 9 of the 17 known black hole binaries that have low-mass donors and $P_{\rm orb} \lesssim 1$ d cannot be produced within the formation scenario we have been evaluating, at least not without some modification of the input physics we have adopted. There are two basic reasons why such low-mass black hole binaries do not form within the context of the model presented. The first has to do with the fact that the orbital energy in primordial binaries with low-mass secondaries is generally insufficient to unbind the envelopes of the massive primaries (see Section 2). The second reason is that we have assumed that once a black hole binary is formed with an intermediate mass donor, such systems do not experience magnetic braking as a source of orbital angular momentum loss. This, in turn, assures that systems with initially intermediate-mass donors will commence Roche-lobe overflow (RLOF) only after undergoing a significant amount of nuclear evolution, subsequent to which the binary evolution necessarily leads to wider orbits – including periods considerably longer than a day. In this section we reevaluate some of our assumptions and relax a number of constraints to determine whether low-mass, compact, black hole binaries can be formed within the standard scenario.

One promising possibility, discussed in Section 2, is that RLOF in the primordial binary might begin while the primary has a radius

between $R_{\rm HG}$ and $R_{\rm max}$, i.e. after it passes the HG and before it reaches its maximum radial extent. During this phase the star is expected to have lost a significant fraction of its mass in a stellar wind, and this would greatly reduce the amount of orbital energy required to remove the residual envelope in a common-envelope phase. However, as also discussed in Section 2, the mass loss tends to make the orbit expand even faster than the primary can expand, and hence RLOF is not likely to occur. In this case, a close binary will not be formed, if it remains bound at all. The calculations that led to this conclusion involved the assumptions that (1) the specific angular momentum carried away by the wind of the primary has the same value as that of the primary itself, $j_{\rm p}$, and (2) no significant synchronizing tidal torques act between the expanding primary and the orbit.

If we suppose that a fraction, $f_{\rm w}$, of the stellar wind of the primary is deflected by the secondary and leaves the binary with the larger specific angular momentum of a low-mass secondary, $j_{\rm s}$, then the orbital expansion will be diminished, and may even be reversed. This, in turn, could enable RLOF to occur when the primary has lost a significant fraction of its envelope. We have carried out a series of BPS calculations where the specific angular momentum carried away by the wind of the primary is set equal to

$$j_{\rm w} = (1 - f_{\rm w})j_p + f_{\rm w} j_{\rm s}. \qquad (11)$$

The results for the black hole binary formation rates versus the fraction $f_{\rm w}$ are shown as solid curves in Fig. 8. These were calculated for an assumed, illustrative, fixed value of $\lambda = 0.1$. As in Fig. 3 the different curves are for various limits on the mass of the donor star in successfully formed black hole binaries. Note that for $f_{\rm w} = 0$, the results agree with those in Fig. 3, and show that black hole binaries with donors $\lesssim 6\,{\rm M}_\odot$ hardly form with such a small value of $\lambda$. However, as the value of $f_{\rm w}$ is increased by a small amount, e.g. to $\sim$0.05, the formation rates of systems with lower-mass donors grow significantly. For still larger values of $f_{\rm w}$, the formation rates drop back down again. This can be understood as follows. For small values of $f_{\rm w}$ the orbital expansion can be substantially limited, and the primary has a chance to shed a significant part of its envelope before the common-envelope phase. For larger values of $f_{\rm w}$ the orbit actually *shrinks* sufficiently rapidly that RLOF may commence *before* much envelope mass can be lost in a wind. The main problem with this hypothesis (invoking extra angular-momentum loss) is that for lower mass secondaries the fraction of the wind deflected by the secondary goes as the square of the mass ratio, and such fractions are typically much smaller than the values of $f_{\rm w}$ for which this effect is important (however, see, Hachisu, Kato & Nomoto 1999).

We have carried out several other related exploratory tests in which the wind loss rate from the primary was taken to be lower than that given by the Nieuwenhuijzen & de Jager (1990) prescription by factors of 2 and 5. This has a similar effect on inhibiting the orbital widening as discussed above when the specific angular momentum of the wind was enhanced. However, for neither diminution factor of the wind loss rate were a significant number of low-mass black hole binaries formed for any value of $\lambda$.

Finally, in this regard we tested the effects of introducing a strong tidal coupling between the orbit and the rotation of the primary as it evolves to become a giant. We considered the extreme case where the primary remains in corotation with the orbit as it expands through

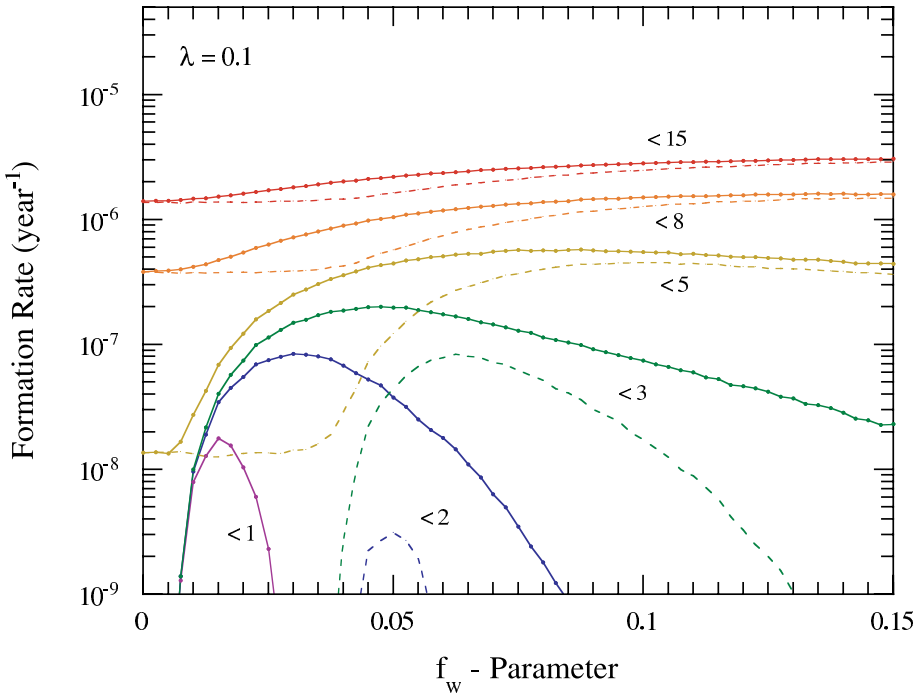


**Figure 8.** Black-hole binary formation rates as a function of the parameter $f_{\rm w}$, the fraction of the primordial primary's stellar wind that is ejected from the binary with the specific angular momentum of the primordial *secondary*. The degree of orbital separation (or contraction) with wind mass loss depends sensitively on this parameter. The remaining fraction $(1 - f_{\rm w})$ is assumed to be lost with the specific angular momentum of the primary. The value of the $\lambda$–parameter has been fixed at an illustrative value of 0.1. Labels on the different curves refer to the maximum mass of the secondary star. Solid curves are *without* the inclusion of tidal interactions between the primary and the orbit. Dashed curves are for an assumed maximum tidal interaction, i.e. the case where the primary always rotates synchronously with the orbit. Note that tidal interactions typically *reduce* the formation rate by tending to bring systems to Roche lobe overflow before the primary has lost sufficient mass to help in the process of unbinding the envelope.

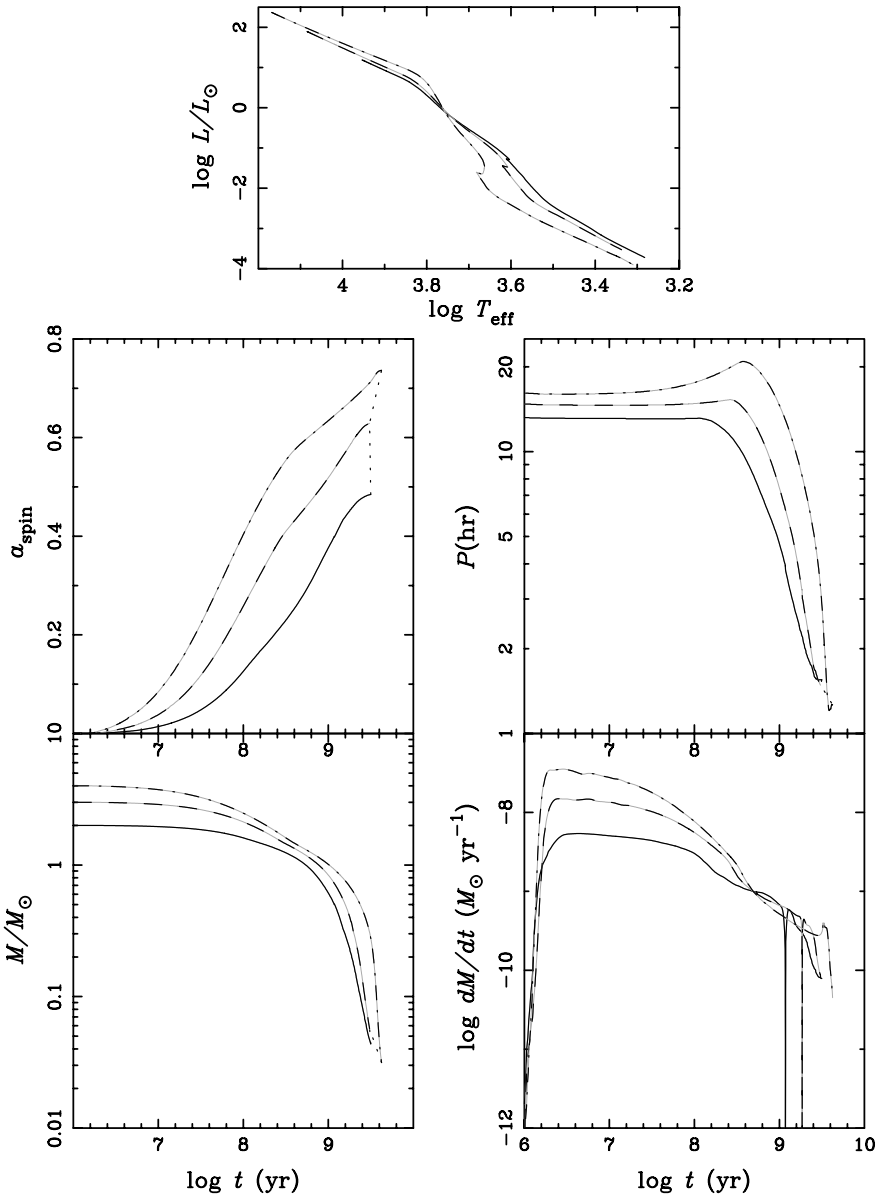


**Figure 9.** HR diagram (top panel) and key binary parameters as a function of time since the beginning of mass transfer (with arbitrary offset) for binary sequences with initial masses of 2 $M_\odot$ (solid curves), 3 $M_\odot$ (dashed curves) and 4 $M_\odot$ (dot–dashed curves) where magnetic braking has been included even for secondaries with radiative envelopes. Middle left: spin parameter. Middle right: orbital period. Bottom left: mass of the secondary. Bottom right: mass-loss rate of the secondary. This figure is available in colour in the online version of the journal on *Synergy*.

the giant phase. This is equivalent to assuming that the tidal synchronization time-scale is always short compared with the nuclear evolution time-scale of the primary – which may not be unreasonable for these largely convective stars (see e.g. Lecar, Wheeler & McKee 1976; Zahn 1977; Verbunt & Phinney 1995). The tidal interactions have the effect of slowing the orbital expansion or causing orbital contraction as the primary's moment of inertia grows, and in the case of low-mass secondaries the Darwin instability is even likely to set in. In the latter case, we simply assume that RLOF commences at that point. The results of our BPS calculations for strong tidal interactions are shown in Fig. 8 as a set of dashed curves (same mass colour coding as for the no tidal interaction case). These represent the formation rates for black hole binaries with different secondary masses – again as a function of the $f_{\rm w}$ parameter discussed above. For systems with higher mass secondaries, the assumed tidal interaction does not significantly change the formation rates. However, for the lower mass secondaries, it is clear that tidal interactions serve only to *decrease* the formation rates, rather than enhance them. This is due to the fact that for small values of $q = M_{\rm s}/M_{\rm p}$, the tidal influence is quite large, leading to either rapid orbital shrinkage or a runaway Darwin instability. This forces an earlier commencement of RLOF and leaves much of the primary's envelope to be ejected in the common envelope.

The net conclusion of these studies is that it is still quite problematic to form low-mass black hole binaries directly via a common-envelope scenario. If, on the other hand, systems with initially intermediate-mass donors could evolve to short orbital periods with low-mass donors, then initially low-mass donors might not be required at all. Indeed, as was shown in PRP, intermediate-mass X-ray binaries containing neutron stars rather than black holes can

be almost indistinguishable from low-mass systems after an initial thermal time-scale mass-transfer phase. Even systems with secondaries as high as 3.5 $M_\odot$ can evolve towards short orbital periods if the secondary is initially relatively unevolved. The reason is that, for intermediate-mass neutron star binaries, mass transfer initially occurs from the more massive to the less massive component of the system which leads to a decrease in the orbital period. When the secondaries develop convective envelopes, magnetic braking becomes the dominant mechanism to drive mass transfer, causing the orbit to shrink further. In the intermediate-mass black hole binaries, the initial mass ratio is reversed and the systems tend to widen from the beginning. This situation would, however, be different if there were an additional angular-momentum loss mechanism operating in these systems.

To test this possibility, we decided to relax our condition for when orbital angular momentum losses via magnetic braking of the donor star are effective. In particular, we investigated how black hole binaries with intermediate-mass donor stars would evolve if magnetic braking were operable, independent of the presence or absence of a convective envelope. In Fig. 9 we show detailed binary evolution results for systems with donor stars of initial mass 2, 3 and 4 $M_\odot$ with the inclusion of continuous magnetic braking. Note that within some $\sim 10^9$ yr of the commencement of mass transfer, the mass of all the donors has been reduced below $\sim 1$ $M_\odot$ and that the orbital periods have decreased from their initial values of $\sim 1/2$ d through a range of several hours. The calculations were terminated when the systems reached their period minimum, which varied from 76 min for the initially 4 $M_\odot$ donor to 93 min for the initially 2-$M_\odot$ donor (the final composition in the former case is significantly hydrogen-depleted and has a hydrogen mass fraction of 0.34, while in the latter case the secondary is only moderately hydrogen depleted).

We have no direct way of evaluating whether conventional ideas about magnetic braking can be overturned in this way or whether there might be some other angular-momentum loss mechanism in order to form the observed low-mass black hole binaries. However, it seems to us to be a more attractive alternative than invoking common-envelope scenarios that implicitly violate conservation of energy.

### 4.5 Discussion and conclusions

In this paper we systematically explored the formation and evolution of black hole binaries. Our binary calculations have shown that mass transfer is stable for a wide range of donor masses (up to about $\sim 20$ $M_\odot$ for an initial black hole mass of 10 $M_\odot$). After sufficient mass has been lost from the donor, an initially intermediate-mass donor can mimic a low-mass one and a high-mass donor can mimic an intermediate-mass one. We have shown that black holes can gain substantial mass from the companion even if accretion is Eddington-limited and that the black hole can be spun up significantly. This demonstrates that the present black hole mass is not necessarily representative of the initial black hole mass after the supernova in which it formed, an important fact to be taken into account when studying the implications of observed black hole masses for single-star evolution.

Our models are directly applicable to many observed black hole binaries, where we particularly concentrated on GRS 1915+105 and Cyg X-1. Our calculations show that the initial mass of the mass donor in GRS 1915+105 may have been as high as $\sim 6$ $M_\odot$ and the black hole may have accreted up to $\sim 4$ $M_\odot$ from its companion, being spun up in the process. The composition of the donor, in particular the helium abundance and the amount of CNO processing it underwent, provides a potentially powerful test of the initial mass of the donor star. V404 Cyg, a massive black hole binary with an orbital period of 6.5 d and some of the best determined system parameters (Shahbaz et al. 1994; Shahbaz et al. 1996), is also very well reproduced by our evolutionary sequences.

Our calculations may also help us to understand the nature of ultraluminous X-ray sources (ULXs) in external galaxies, in particular those found in regions of active star formation. In our massive sequences, the systems reach *potential* X-ray luminosities as high as $\sim 10^{41}$ erg $s^{-1}$, comparable with the most luminous ULXs observed, when the donor stars become giants and the evolution is driven by the nuclear evolution of the hydrogen-burning shell.

We have also performed detailed binary population synthesis calculations which show that intermediate- and high-mass black hole binaries can form at reasonable rates with plausible assumptions, while (initially) low-mass black hole binaries apparently cannot, unless one is prepared to accept violation of energy conservation. We have explored various possible solutions to reconcile this conclusion with the large number of low-mass, short-period black hole binaries observed. These include: (1) The possibility that there are serious flaws in the stellar models of massive, evolved stars, or that changes in the assumptions concerning the ejection of the common envelope should be considered. (2) The assumptions concerning the angular-momentum loss in the stellar wind from the primary have to be changed drastically. (3) Low-mass, short-period systems are in fact descendants of intermediate-mass systems. This requires an additional angular-momentum loss mechanism in systems with intermediate-mass radiative stars (e.g. continuous magnetic braking). (4) Low-mass systems form through one of the alternative evolutionary formation channels suggested, e.g. in a triple scenario or out of the collapsed envelope of a massive star.

Finally, we conclude that before some of these fundamental issues have been resolved, the predictions of binary population synthesis studies of black hole binaries have to be taken with considerable caution.

## ACKNOWLEDGMENTS

We thank E. Pfahl, R. Remillard, P. A. Charles, I. F. Mirabel for extremely helpful discussions and the referee, V. Kalogera, for very useful comments. This work was in part supported by a Royal Society UK-China Joint Project Grant (PhP and ZH), the Chinese National Science Foundation under Grant No. 19925312, 10073009 and NKBRSF No. 19990754 (ZH) and the National Aeronautics and Space Administration under ATP grant NAG5-8368.

## REFERENCES

Abt H. A., Levy S. G., 1978, ApJS, 36, 241
Alexander D. R., Ferguson J. W., 1994, ApJ, 437, 879
Angelini L., Loewenstein M., Mushotzky R. F., 2001, ApJ, 557, L35
Arzoumanian Z., Chernoff D. F., Cordes J. M., 2002, ApJ, 568, 289
Bardeen J. M., 1970, Nat, 226, 64
Beer M. E., Podsiadlowski Ph., 2002, MNRAS, 331, 351
Begelman M. C., 2002, ApJ, 568, 97
Belczynski K., Bulik T., 2002, ApJ, 574, L147
Brandt W. N., Podsiadlowski Ph., 1995, MNRAS, 274, 461
Brandt W. N., Podsiadlowski Ph., Sigurdsson S., 1995, MNRAS, 277, L35
Brown G. E., Lee C.-H., Bethe H. A., 1999, New Astron., 4, 313
Brown G. E., Lee C.-H., Wijers R. A. M. J., Bethe H. A., 2000, Phys. Rep., 333, 471
Brown G. E., Heger A., Langer N., Lee C.-H., Wellstein S., Bethe H. A., 2001, New Astron., 6, 457

Canalizo G., Koenigsberger G., Peña D., Ruiz E., 1995, Rev. Mexicana Astron. Astrofis., 31, 63
Cannizzo J., Wheeler J. C., 1984, ApJS, 55, 367
Cappellaro E., Evans R., Turatto M., 1999, A&A, 351, 459
Castro-Tirado A. J., Brandt S., Lund N., 1992, IAU Circ. 5590
Chevalier R. A., 1993, ApJ, 411, L33
Chiang E., Rappaport S., 1996, ApJ, 469, 255
Colbert E. J. M., Mushotzky R. F., 1999, ApJ, 519, 89
Colbert E. J. M., Ptak A. F., 2002, ApJS, 143, 25
de Kool M., 1990, ApJ, 358, 189
Dewi J., Tauris T., 2000, A&A, 360, 1043
Dewi J., Tauris T., 2001, in Podsiadlowski Ph., Rappaport S., King A. R., D'Antona F., Burderi L., eds, ASP Conf. Ser. Vol. 229, Evolution of Binary and Multiple Stars Systems. Astron. Soc. Pac., San Francisco, p. 255
Duquennoy A., Mayor M., 1991, A&A, 248, 485
Eggleton P. P., Verbunt F., 1986, MNRAS, 220, 13
Ergma E., Fedorova A., 1998, A&A, 338, 69
Ergma E., van den Heuvel E. P. J., 1998, A&A, 331, L29
Fabbiano G., 1989, ARA&A, 27, 87
Fryer C. L., Heger A., 2000, ApJ, 541, 1033
Fryer C. L., Kalogera V., 2001, ApJ, 554, 548
Fryer C. L., Burrows A., Benz W., 1997, ApJ, 496, 333
Garmany C. D., Conti P. S., Massey P., 1980, ApJ, 242, 1063
Gies D. R., Bolton C. T., 1982, ApJ, 260, 240
Gies D. R., Bolton C. T., 1986, ApJ, 304, 371
Gies D. R. et al., 2003, ApJ, 583, 424
Greiner J., Morgan E. H., Remillard R. A., 1996, ApJ, 473, L107
Greiner J., Morgan E. H., Remillard R. A., 1998, New Astron. Rev., 42, 597
Greiner J., Cuby J. G., McCaughrean M. J., 2001, Nat, 414, 522
Hachisu I., Kato M., Nomoto K., 1999, ApJ, 522, 487
Han Z., Podsiadlowski Ph., Eggleton P. P., 1994, MNRAS, 270, 121
Han Z., Podsiadlowski Ph., Maxted P. F. L., Marsh T. R., Ivanova N., 2002, MNRAS, 336, 449
Han Z., Podsiadlowski Ph., Maxted P. F. L., Marsh T. R., 2003, MNRAS, in press
Hansen B. M. S., Phinney E. S., 1997, MNRAS, 291, 569
Herrero A., Kudritzki R. P., Gabler R., Vilchez J. M., Gabler A., 1995, A&A, 297, 556
Hjellming M. S., Webbink R. F., 1987, ApJ, 318, 794
Houck J. C., Chevalier R. A., 1991, ApJ, 376, 234
Hurley J. R., Pols O. R., Tout C. A., 2000, MNRAS, 315, 543 (HPT)
Janka H.-T., Müller E., 1994, A&A, 290, 496
Jeltema J. E., Canizares C. R., Buote, D. A., Garmire G. P., 2002, ApJ, submitted
Kalogera V., 1999, ApJ, 521, 723
Kalogera V., Webbink R. F., 1996, ApJ, 458, 301
Kalogera V., Webbink R. F., 1998, ApJ, 493, 351
Kilgard R. E., Kaaret P., Krauss H. I., Prestwich A. H., Raley M. T., Zezas A., 2002, ApJ, 573, 138
King A. R., 2002, MNRAS, 335, L13
King A. R., Kolb U., 1999, MNRAS, 305, 654
King A. R., Kolb U., Szuskiewicz E., 1997, ApJ, 488, 89
King A. R., Davies M. B., Ward M. J., Fabbiano G., Elvis M., 2001, ApJ, 552, L109
Kippenhahn R., Weigert A., 1990, Stellar Structure and Evolution. Springer, Berlin
Kippenhahn R., Weigert A., Hofmeister E., 1967, in Alder B., Fernbach S., Rothenberg M., eds, Methods in Computational Physics. Vol. 7, p. 129
Kundu A., Maccarone T. J., Zepf S. E., 2002, ApJ, 574, L5
Lai D., Chernoff D. F., Cordes J. M., 2001, ApJ, 549, 1111
Langer N., Maeder A., 1995, A&A, 295, 685
Lasota J.-P., 2002, New Astron. Rev., 45, 449
Lecar M., Wheeler J. C., McKee C. F., 1976, ApJ, 205, 556
Lee C.-H., Brown G. E., Wijers R. A. M. J., 2002, ApJ, 575, L996 (LBW)
Levine A., Rappaport S., Putney A., Corbet R., Nagase F., 1991, ApJ, 381, 101
Levine A., Rappaport S., Deeter J., Boynton P., Nagase F., 1993, ApJ, 410, 328
Lira P., Johnson R., Lawrence A., 2002, MNRAS, submitted (astro-ph/0206123)
Lyne A. G., Lorimer D. R., 1994, Nat, 369, 127
Maeder A., 1992, A&A, 264, 105
Makishima K. et al., 2000, ApJ, 535, 632
Miller G. E., Scalo J. M., 1979, ApJS, 41, 513
Mirabel I. F., Rodríguez L. F., 1994, Nat, 371, 46
Mirabel I. F., Rodríguez L. F., 1999, ARA&A, 37, 409
Nelemans G., van den Heuvel E. P. J., 2001, A&A, 376, 950
Nelemans G., Tauris T. M., van den Heuvel E. P. J., 1999, A&A, 352, 87
Nieuwenhuijzen H., de Jager C., 1990, A&A, 231, 134
Nugis T., Lamers H. J. G. L. M., 2000, A&A, 360, 227
Orosz J. A. et al., 2002, ApJ, 568, 845
Paczyński B., 1976, in Eggleton P. P., Mitton S., Whelan J., eds, Structure and Evolution of Close Binaries. Kluwer, Dordrecht, p. 75
Pakull M., Mirioni L., 2002, in Jansen F. et al., eds, New Visions of the X-ray Universe in the XMM-Newton and Chandra Era, 26-30 (astro-ph/0202488)
Pfahl E., Rappaport S., Podsiadlowski Ph., Spruit H., 2002, ApJ, 574, 364
Plavec M., 1968, Adv. Astron. Astrophys., 6, 201
Podsiadlowski Ph., 2001, in Podsiadlowski Ph., Rappaport S., King A. R., D'Antona F., Burderi L., eds, ASP Conf. Ser. Vol. 229, Evolution of Binary and Multiple Star Systems. Astron. Soc. Pac., p. 239
Podsiadlowski Ph., Rappaport S., 2000, ApJ, 529, 946
Podsiadlowski Ph., Cannon R. C., Rees M. J., 1995, MNRAS, 274, 485
Podsiadlowski Ph., Nomoto K., Maeda K., Nakamura T., Mazzali P., Schmidt B., 2002a, ApJ, 567, 491
Podsiadlowski Ph., Rappaport S., Pfahl E., 2002b, ApJ, 565, 1107 (PRP)
Pols O. R., Dewi J. D. M., 2002, PASA, 19, 233
Pols O. R., Tout C. A., Schröder K.-P., Eggleton P. P., Manners J., 1997, MNRAS, 289, 869
Portegies Zwart S. F., Verbunt F., Ergma E., 1997, A&A, 321, 207
Rappaport S., Verbunt F., Joss P. C., 1983, ApJ, 275, 713
Ritter H., 1996, in Wijers R. A. M. J., Davies M. B., Tout C. A., eds, Evolutionary Processes in Binary Stars. Kluwer, Dordrecht, p. 223
Roberts T. P., Warwick R. S., 2000, MNRAS, 315, 98
Roberts T. P., Goad M. R., Ward M. J., Warwick R. S., Lira P., 2002, in Jansen F. et al., eds, New Visions of the X-ray Universe in the XMM-Newton and Chandra Era, in press (astro-ph/0202017)
Rogers F. J., Iglesias C. A., 1992, ApJS, 79, 507
Romani R. W., 1992, ApJ, 399, 621
Romani R. W., 1998, A&A, 333, 583
Salpeter E. E., 1955, ApJ, 121, 161
Sazonov S. Y., Sunyaev R. A., Lapshov I. Y., Lund N., Brandt S., Castro-Tirado A., 1994, Astron. Lett., 20, 787
Schröder K.-P., Pols O. R., Eggleton P. P., 1997, MNRAS, 285, 696
Shahbaz T., Ringwald F. A., Bunn J. C., Naylor T., Charles P. A., Casares J., 1994, MNRAS, 271, L10
Shahbaz T., Bandyopadhyay R., Charles P. A., Naylor T., 1996, MNRAS, 282, 977
Sowers J. W., Gies D. R., Bagnuolo G., Jr, Shafter A. W., Wiemker R., Wiggs M. S., 1998, ApJ, 506, 424
Spruit H. C., Phinney E. S., 1998, Nat, 393, 139
Straiys V., Kuriliene G., 1981, Ap&SS, 80, 353
Taam R. E., Sandquist E. L., 2000, ARA&A, 38, 113
Tauris T. M., Dewi J. D. M., 2001, A&A, 369, 170
Terashima Y., Wilson A. S., 2002, in Jansen F. et al., eds, New Visions of the X-ray Universe in the XMM-Newton and Chandra Era. in press (astro-ph/0204321)
Thorne K. S., 1974, ApJ, 191, 507
van den Heuvel E. P. J., 2001, in Podsiadlowski Ph., Rappaport S., King A. R., D'Antona F., Burderi L., eds, ASP Conf. Ser. Vol. 229, Evolution of Binary and Multiple Star Systems. Astron. Soc. Pac., San Francisco, p. 525
van den Heuvel E. P. J., Portegies Zwart S. F., Bhattacharya D., Kaper L., 2000, A&A, 364, 563

van Paradijs J., 1996, ApJ, 464, L139
Verbunt F., Phinney E. S., 1995, A&A, 296, 709
Verbunt F., van den Heuvel E. P. J., 1995, in Lewin W. H. G., van Paradijs J., van den Heuvel E. P. J., eds, X-ray Binaries. Cambridge Univ. Press, Cambridge, p. 457
Verbunt F., Zwaan C., 1981, A&A, 100, L7
Vilhu O., 2002, A&A, 388, 936
Vrtilek S. D., Raymond J. C., Garcia M. R., Verbunt F., Hasinger G., Kurster M., 1990, A&A, 235, 162
Walborn N. R., 1973, ApJ, 179, L123
Wellstein S., Langer N., 1999, A&A, 350, 148
White N. E., van Paradijs J., 1996, ApJ, 473, L25
White R. E., III, Sarazin C. L., Kulkarni S. R., 2002, ApJ, 571, L23
Wijers R. A. M. J., 1996, in Wijers R. A. M. J., Davies M. B., Tout C. A., eds, Evolutionary Processes in Binary Stars. Kluwer, Dordrecht, p. 327
Woosley S. E., Weaver T. A., 1995, ApJS, 101, 181
Woosley S. E., Langer N., Weaver T. A., 1995, ApJ, 448, 315
Zahn J.-P., 1977, A&A, 57, 383
Zezas A., Fabbiano G., Rots A. H., Murray S. S., 2002, ApJ, 577, 710
Zhang S. N., Cui W., Chen W., 1997, ApJ, 482, L155

This paper has been typeset from a TEX/LATEX file prepared by the author.